SRNL-STI-2009-00180
REVISION 0

Key Words:
Tank 12
Characterization
Al Dissolution

Retention:
Permanent

TANK 12 SLUDGE CHARACTERIZATION AND ALUMINUM DISSOLUTION DEMONSTRATION

S. H. Reboul
M. S. Hay
K. E. Zeigler
M. E. Stone

MARCH 2009

Savannah River National Laboratory
Savannah River Nuclear Solutions
Aiken, SC 29808

Prepared for the U.S. Department of Energy Under Contract Number DE-AC09-08SR22470

SRNL
SAVANNAH RIVER NATIONAL LABORATORY

DISCLAIMER

Printed in the United States of America

Prepared for
U.S. Department of Energy

SRNL-STI-2009-00180
REVISION 0

Key Words:
Tank 12
Characterization
Al Dissolution

Retention:
Permanent

TANK 12 SLUDGE CHARACTERIZATION AND ALUMINUM DISSOLUTION DEMONSTRATION

S. H. Reboul
M. S. Hay
K. E. Zeigler
M. E. Stone

MARCH 2009

Savannah River National Laboratory
Savannah River Nuclear Solutions
Savannah River Site
Aiken, SC 29808

Prepared for the U.S. Department of Energy Under
Contract Number DE-AC09-08SR22470

SRNL
SAVANNAH RIVER NATIONAL LABORATORY
TM

REVIEWS AND APPROVALS

S. H. Reboul, Co-author, Process Engineering Technology Date

M. S. Hay, Co-author, Advanced Characterization and Processing Date

K. E. Zeigler, Co-author, Spectroscopy and Separations Date

M. E. Stone, Co-author, Process Engineering Technology Date

J. M. Pareizs, Technical Reviewer, Process Engineering Technology Date

M. T. Keefer, Manager, Sludge Batch 6 Project Owner Date

J. E. Occhipinti, Manager, Waste Solidification Engineering Date

C. C. Herman, Manager, Process Engineering Technology Date

S. L. Marra, Manager, Environmental & Chemical Process Technology Research Programs Date

TABLE OF CONTENTS

LIST OF FIGURES

LIST OF TABLES

LIST OF ACRONYMS

AA	Atomic Absorption
AR	Aqua Regia
AS	Alpha Spectroscopy
AU	Analytical Uncertainty
BT	Base Titration
CLC	Calculated
CS	Chemical Separation
DR	Dissolution Rate
DWPF	Defense Waste Processing Facility
GS	Gamma Spectroscopy
HDPE	High Density Polyethylene
IC	Ion Chromatography
ICP-AES	Inductively Coupled Plasma – Atomic Emission Spectroscopy
ICP-MS	Inductively Coupled Plasma – Mass Spectroscopy
LSC	Liquid Scintillation Counting
LTAD	Low Temperature Aluminum Dissolution
PF	Peroxide Fusion
RM	Rheology Measurement
SME	Slurry Mix Evaporator
SRAT	Sludge Receipt and Adjustment Tank
TIC	Total Inorganic Carbon
TTQAP	Task Technical and Quality Assurance Plan
TTR	Task Technical Request
VWM	Volume Weight Measurement
WDW	Wet and Dry Weight
XRD	X-ray Diffraction

1.0 EXECUTIVE SUMMARY

A 3-L sludge slurry sample from Tank 12 was characterized and then processed through an aluminum dissolution demonstration. The dominant constituent of the sludge was found to be aluminum in the form of boehmite. The iron content was minor, about one-tenth that of the aluminum. The salt content of the supernatant was relatively high, with a sodium concentration of ~7 M. Due to these characteristics, the yield stress and plastic viscosity of the unprocessed slurry were relatively high (19 Pa and 27 cP), and the settling rate of the sludge was relatively low (~20% settling over a two and a half week period).

Prior to performing aluminum dissolution, plutonium and gadolinium were added to the slurry to simulate receipt of plutonium waste from H-Canyon. Aluminum dissolution was performed over a 26 day period at a temperature of 65 ºC. Approximately 60% of the insoluble aluminum dissolved during the demonstration, with the rate of dissolution slowing significantly by the end of the demonstration period. In contrast, approximately 20% of the plutonium and less than 1% of the gadolinium partitioned to the liquid phase. However, about a third of the liquid phase plutonium became solubilized prior to the dissolution period, when the H-Canyon plutonium/gadolinium simulant was added to the Tank 12 slurry. Quantification of iron dissolution was less clear, but appeared to be on the order of 1% based on the majority of data (a minor portion of the data suggested iron dissolution could be as high as 10%).

The yield stress of the post-dissolution slurry (2.5 Pa) was an order of magnitude lower than the initial slurry, due most likely to the reduced insoluble solids content caused by aluminum dissolution. In contrast, the plastic viscosity remained unchanged (27 cP). The settling rate of the post-dissolution slurry was higher than the initial slurry, but still relatively low compared to settling of typical high iron content/low salt content sludges. Approximately 40% of the post-dissolution sludge settled over a three week period. The corresponding volume of supernatant that was decanted from the waste was approximately 35% of the total waste volume. The decanted supernatant contained approximately one-third of the dissolved aluminum and exhibited a mild greenish-grey hue.

2.0 INTRODUCTION

Aluminum dissolution is used to reduce the mass of sludge dispositioned to the Defense Waste Processing Facility (DWPF). During aluminum dissolution, free hydroxide converts solid phase gibbsite [$Al(OH)_3$] and boehmite [AlO(OH)] to liquid phase aluminate ($NaAlO_2$),[1] which is separated from sludge via washing and decanting. The net result is a reduction in the mass of sludge sent to DWPF, with a corresponding decrease in canister production.

A laboratory demonstration of the Low Temperature Aluminum Dissolution (LTAD) process was performed at SRNL in 2007, using a three liter sludge sample taken from Tank 51 before blending with Tank 7 waste to form Sludge Batch 5. This demonstration was conducted at a temperature of 55 ºC, over a 21 day period, and provided a basis for gauging dissolution effectiveness (~ 40% of the aluminum dissolved) and potential downstream impacts[2,3,4].

Subsequently, LTAD was performed in Tank 51, under temperature conditions ranging from 55-64 ºC and a dissolution period of 46 days. Data from this in-tank processing suggested that the higher temperatures and longer duration increased the aluminum dissolution effectiveness, as ~60% of the aluminum dissolved under the in-tank conditions.[5] Additionally, the data from this demonstration[6,7] provided a basis for identifying potential downstream impacts at DWPF.

In this document, a lab-scale demonstration focusing on characterization and aluminum dissolution of Tank 12 sludge, which is a primary component of Sludge Batches 6 and 7, is addressed. This aluminum dissolution demonstration was conducted: a) on a three liter sludge sample taken from Tank 12; b) at a temperature of 65 ºC; c) with Pu/Gd added to the sludge to represent receipt of waste from the H-Canyon discards program; and d) over a dissolution period of 26 days. Effectiveness of aluminum dissolution, solubility/separation of Pu and Gd, and potential process impacts associated with dissolution of the Tank 12 sludge were the primary focus areas of the demonstration.

This work was performed at the request of the Waste Processing Technology Development group of the Liquid Waste Organization (HLE-TTR-2008-52).[8]

3.0 OBJECTIVES

The overall goal of the demonstration was to provide data supporting efficient disposition of the Tank 12 sludge. The specific objectives were:

1) Characterize the Tank 12 sludge sufficiently to provide data for LWO's waste transfer needs, aluminum dissolution flowsheet support, and sludge batch planning;

2) Quantify the aluminum dissolution effectiveness as a function of time;

3) Determine the impact of aluminum dissolution on: a) solid-liquid phase partitioning of Pu and Gd; b) rheology of sludge; and c) settling rate of insoluble solids;

4) Identify other chemical and physical characteristics that are impacted by dissolution.

4.0 QUALITY ASSURANCE

This demonstration was conducted in accordance with the quality assurance protocols identified in the Task Technical and Quality Assurance Plan (TTQAP, SRNS-RP-2008-00156).[9] All of the raw data and ancillary information related to this demonstration were recorded in laboratory notebooks WSRC-NB-2008-00077, WSRC-NB-2008-00078, and SRNL-NB-2009-00021.[10,11,12] A detailed breakdown of the analyses performed during the various phases of the demonstration is given in the Analytical Study Plan (SRNL-RP-2008-00171).[13]

5.0 METHODOLOGY

5.1 SAMPLE DESCRIPTION

A 3-L sludge slurry sample from Tank 12 (HTF-12-08-112) was provided by LWO for the purposes of this demonstration. The sample was received at SRNL on September 3, 2008. The slurry was transferred from the steel sampling vessel to a 1-gal high density polyethylene (HDPE) container, via pumping. After transferring 1.0-1.5 liters of the slurry into the HDPE container, pumping was stopped, while the material remaining in the steel sampling vessel was agitated to facilitate suspension of settled insoluble solids. Pumping was then continued until the steel vessel was essentially empty. The transferred slurry in the HDPE container was allowed to settle over the weekend, after which time a small volume of clear supernatant was transferred back to the steel sampling vessel to rinse out the remaining sludge solids. The rinsate solution containing the residual solids was then transferred back to the HDPE container. A total of 4089 g (3.03 L) of material was recovered from the steel sampling vessel.

5.2 INITIAL SAMPLE CHARACTERIZATION

Approximately 500 mL of the "as received" slurry was utilized for characterization. This material was removed from the 3-L sample after agitating the slurry for approximately 15 minutes using an electrical overhead mixer. Physical measurements of density, solids distribution, and rheology were performed in the SRNL Shielded Cells. All other analyses were performed outside of the cells, by Analytical Development, after performing the initial sample prep activities within the cells. Unless otherwise noted, all analyses were performed in quadruplicate. Summaries of the various preparation and measurement methods are given below.

Generation of supernatant: Following mixing, approximately 200 mL of the 500 mL slurry subsample was filtered through a 0.45 μm porosity membrane to generate supernatant. Portions of the supernatant were retained "as is" for density and dissolved solids measurements. Other portions were prepared for metal and radiological analyses via a) acidification to prevent loss of analytes through sorption onto container walls and minimize precipitation of solids and b) dilution to reduce the dose rates. Additional portions of supernatant were prepared for free hydroxide, carbonate, and other anion analyses via dilution only (to reduce the dose rates). The dilution factors were approximately ten.

Density: Slurry and supernatant densities were determined using volume/weight measurements (VWM) at temperatures of approximately 20 ºC. These temperatures were governed by the Shielded Cells conditions at the time of the measurements. Weight-calibrated balances and 8.2 mL volume-calibrated plastic pipette tips were utilized in the measurements.

Solids distribution: Total solids and dissolved solids contents were determined by performing wet and dry weight (WDW) measurements of slurry and supernatant aliquots, and quantifying the respective ratios of dry weight to wet weight. Dry weights were

measured after driving water from the samples at a nominal temperature of 100-110 ºC (required drying times were 4-5 days for the slurry aliquots and 1-2 days for the supernatant aliquots). The mass of each aliquot (prior to any drying) was ~3.0 g. Insoluble solids content and soluble solids content were then calculated (CLC) based on the total solids and dissolved solids measurements. The calcined solids content was not determined because of the sludge's high sodium salt content (high soluble solids), which made calcined solids measurements impractical. This impracticality was due to instability of the calcined sodium oxides yielding mass measurements that changed drastically over a short period of time.

Rheology: Yield stresses and plastic viscosities of the sludge slurry were determined by generating "flow curves" of shear stress as a function of shear rate. The data for the flow curves was acquired using a Haake RV-30 viscometer at a temperature of 25 ºC. The shear rate was increased from 0-600/s over a five minute period, held at 600/s for one minute, and then reduced from 600-0/s over a five minute period. The yield stress was identified by extrapolating the linear portion of the flow curve back to the Y-axis. The plastic viscosity was identified by calculating the slope of the linear portion of the curve. A total of two rheology measurements (RM) were performed on a single 50-60 mL sample aliquot.

Digestion of slurry samples: In preparation for metal and radiological analyses, slurry samples were digested by two methods: 1) sodium peroxide (PF) fusion; and 2) aqua regia (AR) dissolution. For both methods, a slurry aliquot mass of ~0.7 g was utilized in each digestion. The sodium peroxide fusion was performed in a zirconium crucible at a nominal temperature of 675 ºC after first drying the slurry overnight at a temperature of 110 ºC. The aqua regia dissolution was performed in a Teflon digestion bottle at a nominal temperature of 110 ºC. In both cases, the volume of final digest solution was 250 mL.

Metals: Elemental concentrations of most metals were determined by inductively coupled plasma-atomic emission (ICP-AES) spectroscopy. These analyses were performed on slurry samples digested by both PF and AR, and on acidified diluted supernatant. Isotopic concentrations of various metals and radionuclides were determined by inductively coupled plasma-mass spectroscopy (ICP-MS). These analyses were performed on slurry samples digested by AR and on acidified diluted supernatant. The primary metals and radioisotopes determined by ICP-MS were gadolinium, palladium, ruthenium, rhodium, Tc-99, Th-232, U-235, U-238, Np-237, and Pu-239. Mercury concentrations were determined by cold vapor atomic absorption (AA) spectroscopy. Mercury analysis was performed on slurry samples digested by AR and on unacidified diluted supernatant.

Radiological analyses: Concentrations of important alpha, beta, and gamma-emitting radionuclides were measured by various counting methods. Total alpha and beta activity was determined by pulse-shape discriminating liquid scintillation counting (LSC). Cs-137/Ba-137m activity was determined using gamma spectroscopy (GS). Less dominant gamma-emitters were determined by removing cesium via chemical separation and then performing GS. Sr-90 activity was determined by removing other beta activity via chemical separation and then performing LSC. Isotopic plutonium activities were determined by removing interferences via chemical separation (CS), and then performing alpha spectroscopy (AS) and LSC. U-232 and U-233/234 activities were determined by removing interferences via

chemical separation, and then performing AS. All these analyses were performed on slurry samples digested by PF, and on acidified diluted supernatant.

Gibbsite-boehmite: Speciation of aluminum in insoluble sludge solids was determined using two methods: 1) comparing the dissolution rate (DR) of aluminum in the insoluble solids to that of aluminum in pure gibbsite and that of aluminum in pure boehmite; and 2) x-ray diffraction (XRD) analysis of the insoluble solids. In both methods, the insoluble sludge solids were obtained by filtering the slurry and rinsing the filtered solids with deionized water to remove residual supernatant. The rinsed filtered solids were air-dried prior to proceeding with the speciation analyses.

Free hydroxide, carbonate, and other supernatant anions: Free hydroxide was determined through base titration (BT); carbonate was determined by total inorganic carbon (TIC) analysis; and nitrate, chloride, sulfate, fluoride, formate, phosphate, and oxalate were determined by ion chromatography (IC). All of these analyses were performed on unacidified diluted supernatant.

5.3 PU/GD SOLUTION

A Pu/Gd solution similar to H-canyon's anticipated Pu/Gd waste stream (to be added to Sludge Batch 6) was prepared by a researcher in the Actinide Science Programs group of SRNL. The targeted composition was:

- 4 M nitric acid
- 1 gram plutonium per liter
- 1 gram gadolinium per liter
- 0.1 M potassium fluoride

A total of one liter of the Pu/Gd solution was generated. This volume provided sufficient material for doping the sludge slurry sample such that the final plutonium content would correspond with the proposed limit for High Level Waste vitrified waste forms (5400 grams of plutonium per cubic meter of glass[14]).

Aliquots of the acidic Pu/Gd solution were submitted for analysis, to confirm the composition was consistent with expectations. The following analyses were performed: a) Cs-137, Pu-239, Pu-241, and Am-241 determined by GS; b) Th-232, U-235, U-238, and Pu-239 determined by ICP-MS; c) total alpha and beta activity determined by LSC; and d) metals (including Gd) determined by ICP-AES.

As documented in the Task Technical Request (TTR) and TTQAP, the original plan was to dope the sludge with Pu/Gd in two steps – first, by adding ~25% of the Pu/Gd solution prior to performing aluminum dissolution and second, by adding ~75% of the Pu/Gd solution after performing aluminum dissolution but prior to washing. However, due to suspension of the plutonium disposition project, the second plutonium addition (the one where ~75% of the Pu/Gd was to be added) was cancelled. As a consequence, only ~25% Pu/Gd solution was utilized in the demonstration.

Note that the Pu/Gd solution was alkalized prior to the doping. Specifically, ~300 mL of 50 wt% NaOH solution was added to the liter of acidic Pu/Gd solution, to produce ~1.3 L of alkaline Pu/Gd slurry with a supernatant free hydroxide concentration of approximately 1.2 M. This is the free hydroxide concentration targeted by H-Canyon before discharging wastes to the Tank Farm. The Pu and Gd concentrations of the alkalized slurry were approximately 0.77 g/L.

5.4 ALUMINUM DISSOLUTION

A total of 3241 g (2400 mL) of the Tank 12 sludge slurry sample was transferred to the aluminum dissolution reaction vessel, via pumping. A schematic diagram showing the major components of the reaction vessel and the ancillary equipment is given in Figure 1. Mixing was initiated, and then 250 mL of the alkalized Pu/Gd slurry was added to the sludge in the vessel. Note that 250 mL of the Pu/Gd slurry contained approximately 0.19 g Pu-239 (0.012 Ci Pu-239) and 0.19 g gadolinium. After mixing the combined sludge/Pu/Gd material for 30 minutes, ~100 mL of the Pu/Gd-doped slurry was removed for analysis. Small portions of this material were digested by PF and AR per the methods described in Section 5.2. Approximately 65 mL of the removed slurry aliquot was used to generate supernatant (per the method described in Section 5.2). The following analyses were performed on the Pu/Gd-doped slurry digest and supernatant solutions:

- ICP-AES was performed on PF digest, AR digest, and acidified diluted supernatant
- ICP-MS was performed on AR digest and acidified diluted supernatant
- Isotopic Pu analyses were performed on PF digest and acidified diluted supernatant
- BT and IC were performed on unacidified diluted supernatant

While mixing the slurry in the aluminum dissolution vessel, 685 mL of 50 wt% NaOH solution was slowly added to the contents of the vessel. This quantity of NaOH solution was identified through flowsheet modeling[15] and chosen to represent a free hydroxide to insoluble aluminum molar ratio of 4.4 (see Appendix A). Specifically, the NaOH solution was added in increments of ~50 mL over a total duration of approximately 30 minutes. Temperature was monitored during the additions, with the goal of keeping the temperature below 55 ºC throughout the entire addition period. The temperature goal was met, as the highest recorded temperature during the NaOH addition was 37 ºC, which occurred after adding the final portion of NaOH.

While continuing to mix the combined sludge/Pu/Gd/NaOH material, a 15 mL aliquot of the material was removed and filtered to produce a supernatant sample. This sample represented the aluminum dissolution leachate at time zero. The temperature of the sludge in the dissolution vessel was then raised to 65 ºC, over a period of ~5 hours. About one hour before reaching 65 ºC, the slurry temperature was 64 ºC, and another 15 mL aliquot of the material was removed and filtered to produce supernatant. This supernatant sample represented the aluminum dissolution leachate at a time of 4 hours.

Figure 1. Schematic Diagram of Aluminum Dissolution Reaction Vessel and Equipment

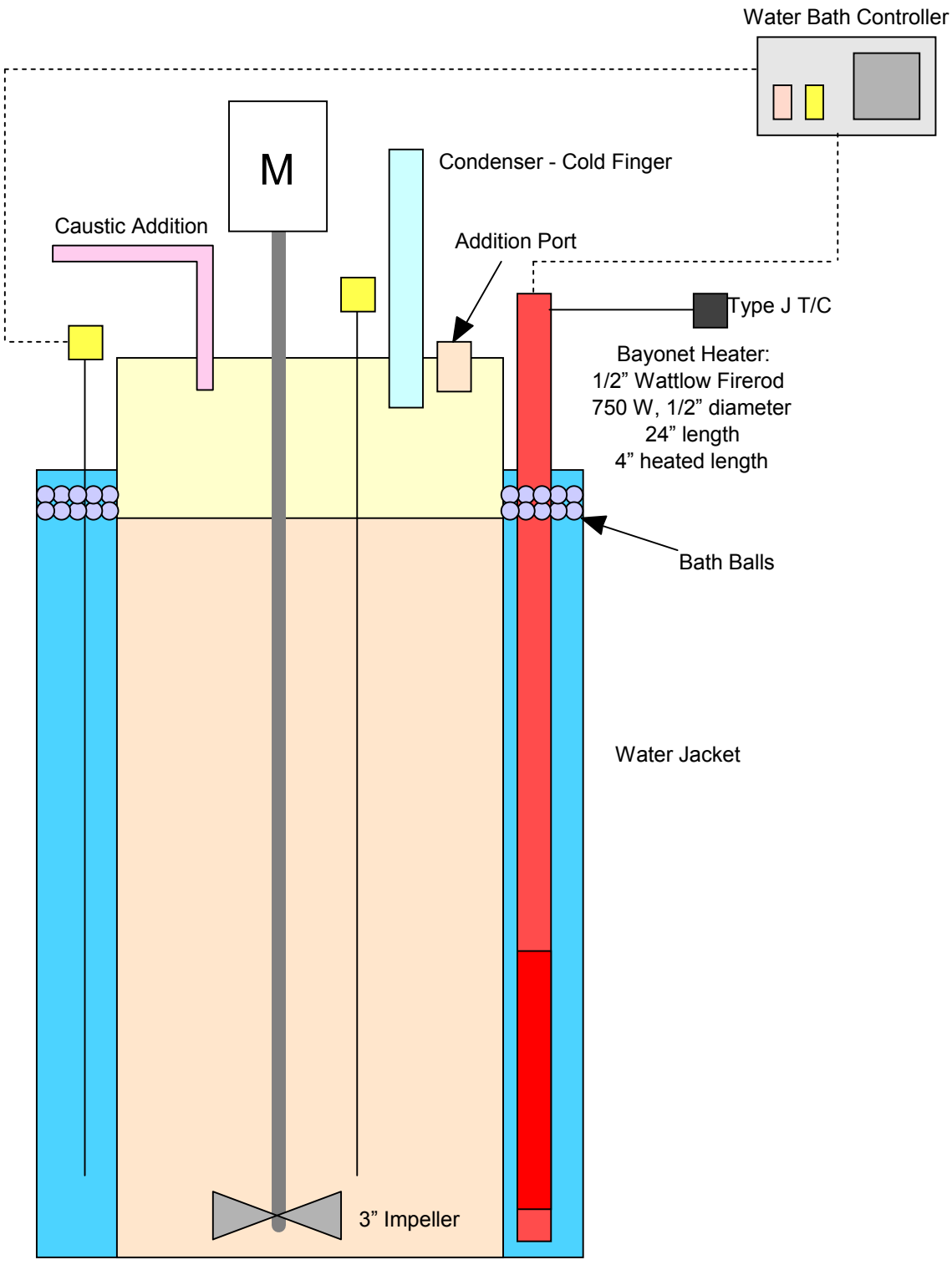

The temperature of the combined sludge/Pu/Gd/NaOH was held at 65 ºC for a total duration of ~26 days. Throughout this period, mixing continued and additional 15 mL samples were removed at the following times: a) 1 day; b) 2 days; c) 5 days; d) 8 days; e) 12 days; f) 15 days; g) 19 days; h) 21 days; and i) 26 days. Each sample was filtered to produce supernatant and represented an aluminum dissolution leachate at a specific time (i.e., 1 day, 2 days, 5 days, etc.). Acidified diluted solutions of the various leachates were submitted for analysis as follows:

- All leachates were submitted for ICP-AES
- All leachates except those from 21 and 26 days were submitted for ICP-MS
- All leachates except those from 12, 15, 19, and 26 days were submitted for AS

The constituents of concern in the leachates included Al, Fe, Gd, U, and Pu. Al concentrations provided a basis for determining aluminum dissolution effectiveness and rate. Fe and Gd concentrations were important from the perspective of identifying solid-liquid phase partitioning of neutron poisons. Similarly, U and Pu concentrations were important from the perspective of identifying solid-liquid phase partitioning of fissile isotopes. Al and Fe were measured by ICP-AES: Gd, U-238, and Pu-239 were measured by ICP-MS; and Pu-238 was measured by AS.

The estimated percentages of the constituents in the liquid phase were computed based on a material balance calculation. This material balance calculation used the solution composition after the addition of the Pu/Gd slurry and the 50 wt% caustic as the starting point (i.e., the time zero solution composition) and the composition of the periodic samples obtained during the aluminum dissolution demonstration as the ending point. This method was used because of inherent uncertainties associated with chemical additions, sampling events, and potential evaporation, which made direct tracking of volume over the course of the demonstration impractical.

At the conclusion of the 26 day aluminum dissolution period, approximately 360 mL of the slurry in the dissolution vessel was removed for analysis. This sample represented the post-dissolution/pre-settling slurry. Just prior to collecting this sample, the mixing speed was increased sufficiently to ensure maximum suspension of insoluble solids which could have settled during the dissolution period. This slurry sample was processed and analyzed for the same set of properties/constituents as the initial slurry sample (Section 5.2), with exception of: a) Sr-90; b) U-232 and U-233/234; and c) gibbsite-boehmite speciation.

5.5 SETTLING OF INSOLUBLE SOLIDS

Following sampling of the "post-dissolution/pre-settling slurry," the mixer was turned off and the temperature setting was reduced to 35 ºC. At this point, the volume of sludge remaining in the dissolution vessel was ~2500 mL. The sludge was allowed to settle for a period of 22 days in the absence of mixing. During this time, the height of the settled sludge layer was monitored at least once per workday, with exception of one workday near the end of the settling period.

Because the post-dissolution supernatant was greenish-grey in color and the walls of the dissolution vessel were semi-opaque, a strong light source needed to be placed behind the vessel and the overhead cell lights dimmed to make the interface between the supernatant layer and the settled sludge layer visible. Unfortunately, the need for this lighting approach was not discovered until the slurry had settled for 45 hours. As a consequence, no useful settling data were acquired prior to this time.

5.6 DECANTING THE SUPERNATANT LAYER FOLLOWING SETTLING

A total of approximately 900 mL of supernatant was decanted from the settled sludge slurry, via pumping. This left approximately 1600 mL of material in the dissolution vessel, of which the top 100 mL (or so) was free supernatant. An aliquot of the decanted supernatant was filtered, acidified/diluted, and submitted for ICP-AES analysis. This sample provided a basis for determining if the metal content of the post-dissolution/post-settling supernatant had changed from that of the post-dissolution/pre-settling supernatant.

5.7 SLUDGE WASHING AND SRAT/SME PROCESSING

As documented in the TTR and TTQAP, the original plan was to wash the post-decant sludge, and then perform Sludge Receipt and Adjustment Tank (SRAT)/Slurry Mix Evaporator (SME) processing. However, due to the suspension of the plutonium disposition project, the sludge washing and SRAT/SME processing parts of the demonstration were cancelled.

6.0 RESULTS AND DISCUSSION

6.1 CHARACTERIZATION OF "AS RECEIVED" SLURRY AND SUPERNATANT

Analytical results for the slurry and the supernatant of the "as received" Tank 12 sample are given in Tables 1 and 2, respectively. These results indicate that the:

- Slurry and supernatant densities were 1.35 and 1.26 g/mL, respectively
- Insoluble solids content was 7.2 wt% and soluble solids was ~32 wt%
- Yield stress and plastic viscosity were relatively high (19 Pa and 27 cP)
- Dominant metal in the insoluble solids was Al and its form was boehmite, as demonstrated through kinetic testing (Appendix B) and XRD spectra (Appendix C)
- Less dominant metals in the insoluble solids included Fe in the form of hematite (Fe_2O_3) and Ca, Mg, and Na present as carbonate salts (see Appendix C)
- Al:Fe ratio was high (about 10:1) and the Fe:Mn ratio was low (about 2:1)
- Gd content was low and its supernatant concentration was undetectable
- Pu-238 was the primary alpha-emitter and 99.9% of it was in the insoluble solids
- Sr-90/Y-90 was the primary beta-emitter in the insoluble solids
- Cs-137 was the primary beta-emitter in supernatant
- Ba-137m was the primary gamma-emitter
- Supernatant contained ~7 M Na^+, 1.5 M free hydroxide, and 0.4 M $Al(OH)_4^-$

Table 1. Analytical Results for the "As Received" Tank 12 Sludge Slurry

Measurement	Method	Mean Result	*%RSD*
Density (g/mL)	VWM	1.35	*1.9*
Total solids (wt% of slurry)	WDW	38.8	*2.3*
Insoluble solids (wt% of slurry)	CLC	7.2	*NA*
Soluble solids (wt% of slurry)	CLC	31.6	*NA*
Yield stress (Pa)	RM	19	*0.3*
Plastic viscosity (cP)	RM	27	*1.0*
Aluminum (wt% of slurry)	PF/ICP-AES	4.2	*4.1*
Boron (wt% of slurry)	AR/ICP-AES	0.0035	*4.7*
Barium (wt% of slurry)	PF/ICP-AES	0.0050	*5.0*
Calcium (wt% of slurry)	AR/ICP-AES	0.085	*4.4*
Cerium (wt% of slurry)	AR/ICP-AES	0.0081	*3.3*
Chromium (wt% of slurry)	PF/ICP-AES	0.014	*9.3*
Copper (wt% of slurry)	PF/ICP-AES	0.0039	*3.2*
Gadolinium (wt% of slurry)	AR/ICP-MS	1.0E-5	*26*
Iron (wt% of slurry)	PF/ICP-AES	0.41	*5.5*
Lanthanum (wt% of slurry)	PF/ICP-AES	0.0043	*11*
Magnesium (wt% of slurry)	AR/ICP-AES	0.081	*4.8*
Manganese (wt% of slurry)	PF/ICP-AES	0.18	*4.4*
Mercury (wt% of slurry)	AR/AA	0.15	*2.3*
Molybdenum (wt% of slurry)	AR/ICP-AES	0.0028	*4.1*
Nickel (wt% of slurry)	PF/ICP-AES	0.047	*4.7*
Palladium (wt% of slurry)	AR/ICP-MS	0.00070	*26*
Potassium (wt% of slurry)	AR/ICP-AES	0.047	*3.0*
Ruthenium (wt% of slurry)	AR/ICP-MS	0.0085	*3.7*
Rhodium (wt% of slurry)	AR/ICP-MS	0.0018	*0.4*
Silicon (wt% of slurry)	AR/ICP-AES	0.016	*2.3*
Silver (wt% of slurry)	AR/ICP-MS	0.00089	*16*
Sodium (wt% of slurry)	AR/ICP-AES	12	*0.4*
Strontium (wt% of slurry)	PF/ICP-AES	0.0027	*8.6*
Thorium (wt% of slurry)	AR/ICP-MS	0.089	*1.8*
Titanium (wt% of slurry)	AR/ICP-AES	0.0011	*1.9*
Uranium (wt% of slurry)	AR/ICP-MS	0.010	*7.4*
Zinc (wt% of slurry)	AR/ICP-AES	0.0054	*1.3*
Zirconium (wt% of slurry)	AR/ICP-AES	0.017	*0.5*
Total alpha (Ci/gallon)	PF/LSC	<0.63	*NA*
Total beta (Ci/gallon)	PF/LSC	11	*3.0*
Co-60 (Ci/gallon)	PF/GS	1.8E-4	*1.2*
Sr-90 (Ci/gallon)	PF/LSC	4.6	*13*
Y-90 (Ci/gallon)	PF/LSC	4.6	*13*
Tc-99 (Ci/gallon)	AR/ICP-MS	7.4E-4	*5.2*
Cs-137 (Ci/gallon)	PF/GS	1.2	*3.3*
Ba-137m (Ci/gallon)	PF/GS	1.1	*3.3*
Eu-152 (Ci/gallon)	PF/GS	8.0E-4	*2.1*
Eu-154 (Ci/gallon)	PF/GS	0.010	*2.3*
Eu-155 (Ci/gallon)	PF/GS	7.1E-4	*8.4*
U-232 (Ci/gallon)	PF/AS	<1.5E-5	*NA*
U-233/234 (Ci/gallon)	PF/AS	1.8E-4	*9.4*
U-235 (Ci/gallon)	AR/ICP-MS	1.2E-7	*5.7*
U-238 (Ci/gallon)	AR/ICP-MS	1.5E-7	*7.4*
Np-237 (Ci/gallon)	AR/ICP-MS	5.6E-6	*28*
Pu-238 (Ci/gallon)	PF/AS	0.26	*3.5*
Pu-239 (Ci/gallon)	AR/ICP-MS	0.0073	*4.8*
Pu-239/240 (Ci/gallon)	PF/AS	0.0063	*9.6*
Pu-241 (Ci/gallon)	PF/LSC	<0.081	*NA*
Am-241 (Ci/gallon)	PF/GS	0.011	*5.3*
Aluminum speciation	DR/XRD	>95% boehmite	*NA*

Table 2. Analytical Results for Filtered Supernatant of the "As Received" Tank 12 Slurry

Measurement	Method	Mean Result	*%RSD*
Density (g/mL)	VWM	1.26	*0.5*
Dissolved solids (wt% of supernatant)	WDW	34.1	*0.5*
Aluminum (mg/L)	ICP-AES	1.1E+4	*0.7*
Boron (mg/L)	ICP-AES	45	*1.0*
Barium (mg/L)	ICP-AES	<0.17	*NA*
Calcium (mg/L)	ICP-AES	29	*4.2*
Cerium (mg/L)	ICP-AES	<4.7	*NA*
Chromium (mg/L)	ICP-AES	1.3E+2	*2.0*
Copper (mg/L)	ICP-AES	1.1	*10*
Gadolinium (mg/L)	ICP-MS	<0.37	*NA*
Iron (mg/L)	ICP-AES	3.0	*6.0*
Lanthanum (mg/L)	ICP-AES	<1.4	*NA*
Magnesium (mg/L)	ICP-AES	31	*1.4*
Manganese (mg/L)	ICP-AES	<0.46	*NA*
Mercury (mg/L)	AA	8.2	*1.7*
Molybdenum (mg/L)	ICP-AES	40	*3.1*
Nickel (mg/L)	ICP-AES	<3.7	*NA*
Palladium (mg/L)	ICP-MS	0.55	*13*
Potassium (mg/L)	ICP-AES	6.6E+2	*2.7*
Ruthenium (mg/L)	ICP-MS	0.72	*35*
Rhodium (mg/L)	ICP-MS	1.4	*7.6*
Silicon (mg/L)	ICP-AES	<4.3	*NA*
Silver (mg/L)	ICP-AES	<2.0	*NA*
Sodium (mg/L)	ICP-AES	1.6E+5	*1.0*
Strontium (mg/L)	ICP-AES	<0.080	*NA*
Thorium (mg/L)	ICP-MS	<0.57	*NA*
Titanium (mg/L)	ICP-AES	<0.29	*NA*
Uranium (mg/L)	ICP-MS	2.3	*5.9*
Zinc (mg/L)	ICP-AES	3.3	*2.9*
Zirconium (mg/L)	ICP-AES	<0.58	*NA*
Total alpha (Ci/gallon)	LSC	<1.7E-4	*NA*
Total beta (Ci/gallon)	LSC	0.40	*0.4*
Sr-90 (Ci/gallon)	LSC	9.5E-4	*15*
Y-90 (Ci/gallon)	LSC	9.5E-4	*15*
Tc-99 (Ci/gallon)	ICP-MS	4.7E-4	*4.7*
Sn-126 (Ci/gallon)	GS	9.5E-7	*2.9*
Sb-126 (Ci/gallon)	GS	9.5E-7	*2.9*
Cs-137 (Ci/gallon)	GS	0.33	*2.4*
Ba-137m (Ci/gallon)	GS	0.31	*2.4*
U-232 (Ci/gallon)	AS	<5.8E-8	*NA*
U-233/234 (Ci/gallon)	AS	2.7E-6	*0.4*
U-235 (Ci/gallon)	ICP-MS	2.9E-9	*28*
U-238 (Ci/gallon)	ICP-MS	2.5E-9	*7.8*
Np-237 (Ci/gallon)	ICP-MS	<1.1E-6	*NA*
Pu-238 (Ci/gallon)	AS	3.1E-4	*1.2*
Pu-239 (Ci/gallon)	ICP-MS	<4.8E-5	*NA*
Pu-239/240 (Ci/gallon)	AS	8.8E-6	*3.3*
Pu-241 (Ci/gallon)	LSC	<8.8E-5	*NA*
Sodium (M)	ICP-AES	7.05	*1.0*
Potassium (M)	ICP-AES	0.017	*2.7*
Free hydroxide (M)	BT	1.53	*1.9*
Nitrite (M)	IC	1.76	*3.7*
Nitrate (M)	IC	1.47	*2.3*
Carbonate (M)	TIC	0.83	*0.6*
Aluminate (M)	ICP-AES	0.39	*0.7*
Chloride (M)	IC	0.025	*1.3*
Sulfate (M)	IC	0.051	*2.2*
Fluoride (M)	IC	<0.016	*NA*
Formate (M)	IC	<0.0069	*NA*
Phosphate (M)	IC	<0.0033	*NA*
Oxalate (M)	IC	<0.0071	*NA*

The data reflect that the Tank 12 slurry: a) was relatively thick; b) contained insolubles comprised almost entirely of boehmite; and c) contained supernatant with a relatively high salt content. Visual observations confirm that the Tank 12 slurry was thick. During transfer of the sample into the labware, the slurry was found to pour and adhere to the labware surfaces much like molasses.

The settling rate of the "as received" sludge was relatively low. After sitting undisturbed (in the absence of mixing) for a period of 19 days, the height of the settled sludge layer was ~82% of the total slurry height. A plot showing the settling behavior as a function of time is given in Figure 2. The relatively high yield stress and low settling rate were attributed to the high aluminum content of the insoluble solids and the high salt content of the supernatant.

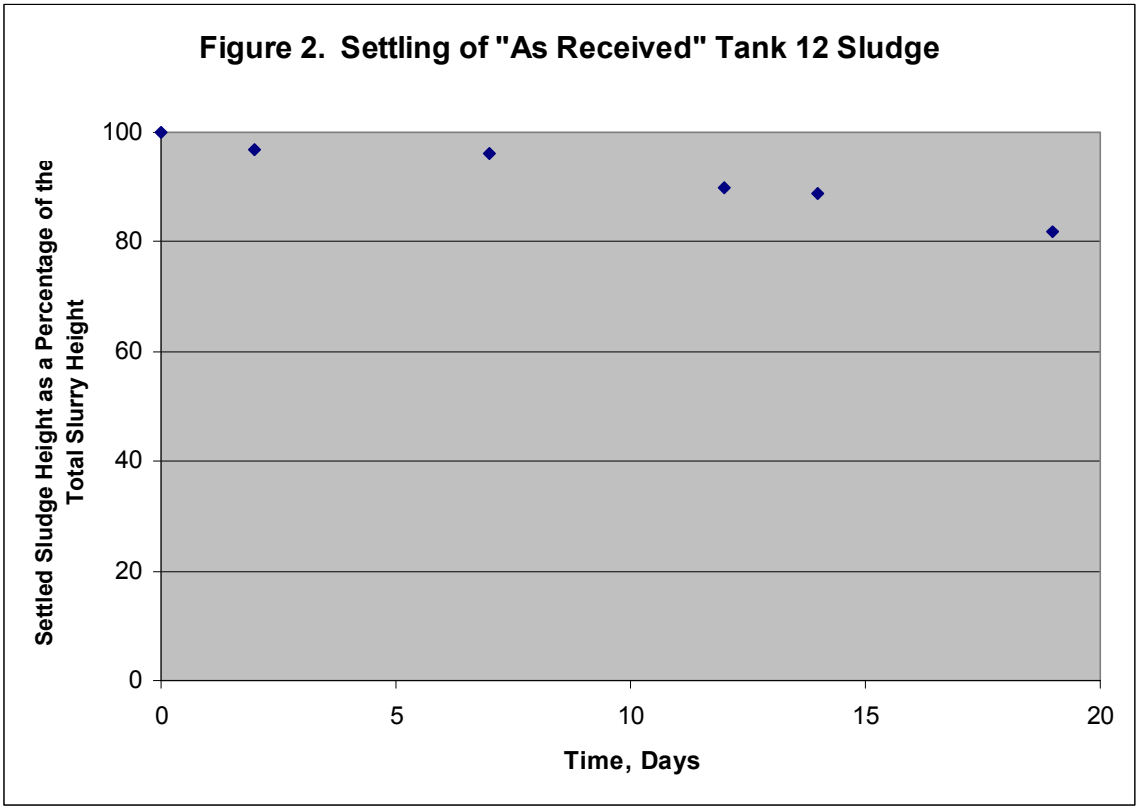

6.2 PU/GD SOLUTION

Analytical results for the acidic Pu/Gd solution are given in Table 3. These results confirmed that the Pu and Gd concentrations were consistent with the targeted values (1.0 g/L). Additionally, the results showed that the concentrations of most other constituents were negligible, with exception of those for Th (170 mg/L), U (3000 mg/L), and Cu (2200 mg/L). Because of the relatively high concentrations of these constituents, the Th, U, and Cu contents of the slurry were raised significantly when the Pu/Gd-doping solution was added.

Table 3. Composition of Acidic Pu/Gd Solution

Constituent	Constituent Concentration	
	mg/L	Ci/gal
Cs-137 (GS)	1.1E-6	3.5E-7
Th-232 (ICP-MS)	1.7E+2	7.2E-8
U-235 (ICP-MS)	2.5E+2	2.1E-6
U-238 (ICP-MS)	2.8E+3	3.6E-6
Pu-239 (ICP-MS)	**9.9E+2**	0.23
Pu-239 (GS)	**9.9E+2**	0.23
Pu-241 (GS)	0.51	0.20
Am-241 (GS)	4.5	0.058
Total alpha activity (LSC)	*NA*	0.30
Total beta activity (LSC)	*NA*	0.15
Boron (ICP-AES)	34	*NA*
Calcium (ICP-AES)	6.1	*NA*
Copper (ICP-AES)	2.2E+3	*NA*
Gadolinium (ICP-AES)	**9.9E+2**	*NA*
Potassium (ICP-AES)	3.7E+3	*NA*
Molybdenum (ICP-AES)	81	*NA*
Sodium (ICP-AES)	60	*NA*
Silicon (ICP-AES)	2.3E+2	*NA*
Titanium (ICP-AES)	22	*NA*
Zinc (ICP-AES)	4.4	*NA*
Zirconium (ICP-AES)	66	*NA*

6.3 PU/GD-DOPED SLURRY AND SUPERNATANT

6.3.1 Slurry

Analytical results for the Pu/Gd-doped slurry are given in Table 4. Some of the results were consistent with expectations and some were not. Results for constituents such as Al, Cr, Fe, Mn, Ni, and Zn were very similar to the results for the pre-doped slurry, which was expected based on the relatively small dilution effect (250 mL Pu/Gd solution added to 2500 mL slurry) and the negligible amount of the these constituents contributed by the Pu/Gd addition. In contrast, results for constituents such as Th, U, and Pu-239 were lower than those of the pre-doped slurry, which was unexpected based on the knowledge that significant amounts of Th, U, and Pu-239 were added, and nothing was done to remove them from the original slurry. An additional example is Gd, where the post-doping concentration was higher than the pre-doping concentration – however, not to the extent that was expected based on the amount of Gd added.

The likely reason for these inconsistencies is two-fold. First is the uncertainty of the analytical data, which for the prevailingly low concentrations of Th, U, and Pu-239 in the demonstration are thought to be significant (20% or greater). An indicator of this uncertainty is observed by comparing the Pu-239 and Pu-239/240 results for the "as received" slurry (Table 1). As seen in the table, the concentration reported for Pu-239 is 0.0073 Ci/gal and the concentration reported for Pu-239/240 is 0.0063 Ci/gal. Obviously the combined Pu-239/240 activity concentration should have been greater than the Pu-239 activity concentration. The difference between the measured concentration for Pu-239/240 and the measured concentration for Pu-239 gives a basis for estimating the uncertainty. If one assumes an isotopic distribution typical for SRS plutonium, the Pu-239/240 result translates to a Pu-239 concentration of around 0.0050 Ci/gal. This is about 30% lower than the Pu-239 measurement, indicating a nominal uncertainty of the same magnitude.

Table 4. Analytical Results for Tank 12 Sludge Slurry Following Addition of Pu/Gd, But Prior to Caustic Addition

Measurement	Method	Mean Result	*%RSD*
Total solids (wt% of slurry)	WDW	35.5	*0.4*
Aluminum (wt% of slurry)	PF/ICP-AES	4.0	*1.4*
Boron (wt% of slurry)	PF/ICP-AES	<0.0065	*NA*
Barium (wt% of slurry)	PF/ICP-AES	0.0050	*3.5*
Calcium (wt% of slurry)	PF/ICP-AES	0.080	*2.1*
Cerium (wt% of slurry)	PF/ICP-AES	<0.012	*NA*
Chromium (wt% of slurry)	PF/ICP-AES	0.013	*4.1*
Copper (wt% of slurry)	PF/ICP-AES	<0.0077	*NA*
Gadolinium (wt% of slurry)	AR/ICP-MS	0.0012	*9.4*
Iron (wt% of slurry)	PF/ICP-AES	0.39	*4.6*
Lanthanum (wt% of slurry)	PF/ICP-AES	<0.0026	*NA*
Magnesium (wt% of slurry)	PF/ICP-AES	0.012	*1.9*
Manganese (wt% of slurry)	PF/ICP-AES	0.17	*2.3*
Molybdenum (wt% of slurry)	PF/ICP-AES	<0.0068	*NA*
Nickel (wt% of slurry)	PF/ICP-AES	0.047	*4.1*
Palladium (wt% of slurry)	AR/ICP-MS	0.00032	*8.9*
Ruthenium (wt% of slurry)	AR/ICP-MS	0.0043	*8.5*
Rhodium (wt% of slurry)	AR/ICP-MS	0.0010	*1.9*
Silicon (wt% of slurry)	PF/ICP-AES	<0.024	*NA*
Silver (wt% of slurry)	AR/ICP-MS	0.00065	*7.9*
Strontium (wt% of slurry)	PF/ICP-AES	<0.0039	*NA*
Thorium (wt% of slurry)	AR/ICP-MS	0.041	*1.6*
Titanium (wt% of slurry)	PF/ICP-AES	<0.0013	*NA*
Uranium (wt% of slurry)	AR/ICP-MS	0.0068	*0.8*
Zinc (wt% of slurry)	PF/ICP-AES	0.0056	*5.5*
Tc-99 (Ci/gallon)	AR/ICP-MS	4.1E-4	*13*
U-235 (Ci/gallon)	AR/ICP-MS	8.2E-8	*5.3*
U-238 (Ci/gallon)	AR/ICP-MS	1.0E-7	*0.7*
Np-237 (Ci/gallon)	AR/ICP-MS	<5.1E-6	*NA*
Pu-238 (Ci/gallon)	PF/AS	<0.25	*NA*
Pu-239 (Ci/gallon)	AR/ICP-MS	0.0059	*3.5*
Pu-239/240 (Ci/gallon)	PF/AS	<0.048	*NA*
Pu-241 (Ci/gallon)	PF/LSC	0.060	*18*

A second reason for the inconsistencies is associated with partitioning of the alkalized Pu/Gd solution and the time necessary for homogenization/equilibration with the Tank 12 slurry. When the Pu/Gd was alkalized, metals were assumed to be precipitated out of solution as hydroxides. The volume of these precipitated hydroxides was small compared to that of the liquid phase, per visual observations. As such, when the Pu/Gd slurry was first introduced into the sludge, the added solids were likely distributed in a relatively small number of sites throughout the slurry and required an extended equilibration time to become uniformly distributed. This explanation is supported by the post-dissolution characterization, which is consistent with expectations (Section 6.5).

Uranium concentrations in the post-doped slurry were about three times those of the “as received” slurry. Increases in the concentrations of plutonium were not as straightforward, due to differences between the various isotopes that were added, detected, and measured. The Pu-238 concentration in the post-doped slurry was about six times that of the pre-doped slurry. Based on the ICP-MS results, the Pu-239 concentration in the post-doped slurry was a minimum of about seven times that of the pre-doped slurry (this increase was identified as a “minimum” because the pre-doped concentration was less than a minimum detection limit).

In contrast, based on the AS results, the Pu-239/240 concentration in the post-doped slurry was fifty times that of pre-doped slurry. This would suggest that the Pu-239 concentration increased by fifty if the ratio of Pu-239 to Pu-240 in the pre-doped slurry were the same as that in the post-doped slurry.

6.3.2 Supernatant

Analytical results for the Pu/Gd-doped supernatant are given in Table 5. These results were consistent with expectations, on the whole. Concentrations of constituents such as Al, Cr, Na, and free hydroxide were very similar to those of the pre-doped supernatant, which was expected based on the relatively small dilution effect and the negligible amount of these constituents contributed by the Pu/Gd addition. In comparison, concentrations of constituents such as Cu, U, and isotopes of Pu were significantly higher than those of the pre-doped supernatant, which was not surprising given their relative abundance in the Pu/Gd solution. Unfortunately, the Gd and Th concentrations were below the minimum detection limits, so conclusions on these constituents could not be discerned.

6.4 DISSOLUTION LEACHATES

Analytical results for the dissolution leachates and the pre- and post-dissolution supernatants are given in Table 6. These results indicate that the dissolution process impacted the constituents of concern to various degrees. A brief discussion of each constituent of concern is given below.

6.4.1 Aluminum

The concentration of Al in solution increased by a factor of about five over the duration of the dissolution period (from 5.4E+3 mg/L at time zero to 2.7E+4 mg/L at t = 26 days). Interestingly, the measured concentration of Al at time zero was about ~30% lower than the value anticipated based upon dilution by the added 50% NaOH. This lower Al concentration may indicate that some precipitation of aluminum occurred between the time the Gd/Pu was added and the start of the dissolution period (t = 0). Also of note is the measured concentration of Al in the post-dissolution supernatant, which is ~10% lower than the concentration observed at the end of the dissolution period (t = 26 days). This lower concentration may be due to analytical uncertainty or it may reflect that a small portion of the Al precipitated out of solution when the material was cooled to the ambient cell temperature (from T = 65 ºC during dissolution to T ≈ 17 ºC following dissolution).

Estimates of the percentages of Al that dissolved over time are given in Figure 3. As shown in the figure, the dissolution rate was highest during the first week or so, and then began leveling off over the remaining period. At t = 8 days, approximately 35% of the Al had dissolved. In contrast, at t = 26 days, approximately 60% of the Al had dissolved.

Table 5. Analytical Results for Filtered Supernatant of Tank 12 Slurry Following Addition of Pu/Gd, But Prior to Caustic Addition

Measurement	Method	Mean Result	*%RSD*
Aluminum (mg/L)	ICP-AES	1.0E+4	*0.3*
Boron (mg/L)	ICP-AES	44	*2.7*
Barium (mg/L)	ICP-AES	<1.5	*NA*
Calcium (mg/L)	ICP-AES	<1.8	*NA*
Cerium (mg/L)	ICP-AES	<23	*NA*
Chromium (mg/L)	ICP-AES	1.3E+2	*0.4*
Copper (mg/L)	ICP-AES	10	*4.1*
Gadolinium (mg/L)	ICP-MS	<1.0	*NA*
Iron (mg/L)	ICP-AES	<3.3	*NA*
Lanthanum (mg/L)	ICP-AES	<3.8	*NA*
Magnesium (mg/L)	ICP-AES	<0.51	*NA*
Manganese (mg/L)	ICP-AES	<0.73	*NA*
Molybdenum (mg/L)	ICP-AES	37	*6.6*
Nickel (mg/L)	ICP-AES	<37	*NA*
Palladium (mg/L)	ICP-MS	0.55	*28*
Potassium (mg/L)	ICP-AES	6.4E+2	*1.1*
Ruthenium (mg/L)	ICP-MS	<2.4	*NA*
Rhodium (mg/L)	ICP-MS	1.6	*3.9*
Silicon (mg/L)	ICP-AES	<35	*NA*
Silver (mg/L)	ICP-AES	<6.4	*NA*
Sodium (mg/L)	ICP-AES	1.5E+5	*0.3*
Strontium (mg/L)	ICP-AES	<0.34	*NA*
Thorium (mg/L)	ICP-MS	<0.78	*NA*
Titanium (mg/L)	ICP-AES	<1.9	*NA*
Uranium (mg/L)	ICP-MS	7.0	*2.6*
Zinc (mg/L)	ICP-AES	<4.5	*NA*
Zirconium (mg/L)	ICP-AES	<1.5	*NA*
Tc-99 (Ci/gallon)	ICP-MS	4.5E-4	*2.9*
U-235 (Ci/gallon)	ICP-MS	6.1E-9	*26*
U-238 (Ci/gallon)	ICP-MS	7.9E-9	*2.6*
Np-237 (Ci/gallon)	ICP-MS	<3.8E-7	*NA*
Pu-238 (Ci/gallon)	AS	1.9E-3	*4.3*
Pu-239 (Ci/gallon)	ICP-MS	3.3E-4	*7.3*
Pu-239/240 (Ci/gallon)	AS	4.4E-4	*6.7*
Pu-241 (Ci/gallon)	LSC	<1.5E-3	*NA*
Sodium (M)	ICP-AES	6.69	*0.3*
Potassium (M)	ICP-AES	0.016	*1.1*
Free hydroxide (M)	BT	1.56	*0.9*
Nitrite (M)	IC	1.34	*2.5*
Nitrate (M)	IC	1.21	*2.1*
Carbonate (M)	CLC from BT	0.80	*NA*
Aluminate (M)	ICP-AES	0.38	*0.3*
Chloride (M)	IC	0.019	*1.0*
Sulfate (M)	IC	0.058	*4.2*
Fluoride (M)	IC	<0.018	*NA*
Formate (M)	IC	<0.0078	*NA*
Phosphate (M)	IC	<0.0037	*NA*
Oxalate (M)	IC	<0.0040	*NA*

Table 6. Liquid Phase Constituent Concentrations Before, During, and After Aluminum Dissolution

Sample	Supernatant Constituent Concentration, mg/L					
	Al	Fe	Gd	U-238	Pu-238	Pu-239
As rec'd supernatant	1.1E+4	3.0	<0.4	2.0	0.0048	<0.20
Supernatant after adding Pu/Gd	1.0E+4	<3.3	<1.0	6.3	0.030	1.4
Dissolution leachate, t=0	5.4E+3	11	<0.9	5.8	0.045	7.3
Dissolution leachate, t=4 h	6.5E+3	10	<0.9	11	0.097	19
Dissolution leachate, t=1 d	8.6E+3	12	<1.3	8.8	0.11	17
Dissolution leachate, t=2 d	1.1E+4	15	<1.1	8.9	0.10	18
Dissolution leachate, t=5 d	1.5E+4	24	<1.0	7.1	0.10	17
Dissolution leachate, t=8 d	1.9E+4	38	<1.6	6.2	0.12	20
Dissolution leachate, t=12 d	2.0E+4	240	<0.9	6.0	NM	16
Dissolution leachate, t=15 d	2.4E+4	25	<1.3	5.9	NM	17
Dissolution leachate, t=19 d	2.3E+4	35	<1.0	5.4	NM	17
Dissolution leachate, t=21 d	2.6E+4	110	<0.6	NM	0.13	NM
Dissolution leachate, t=26 d	2.7E+4	370	<0.6	NM	NM	NM
Post-diss. supernatant, T≈17 ºC	2.4E+4	21*	<1.7	4.4	0.095	12

*Note: 21 mg/L is the Fe concentration result obtained for the filtrate of the final decant solution, not the post-dissolution supernatant (the supernatant filtered from the slurry). The decant solution result for Fe was reported in Table 6 because the measured concentration for the post-dissolution supernatant was less than an unusually high minimum detection limit (<100 mg/L). Comparison of the analytical results for the final decant solution (Table 13) and the post-dissolution supernatant (Table 9) indicate the two solutions were very similar from a metals content perspective.

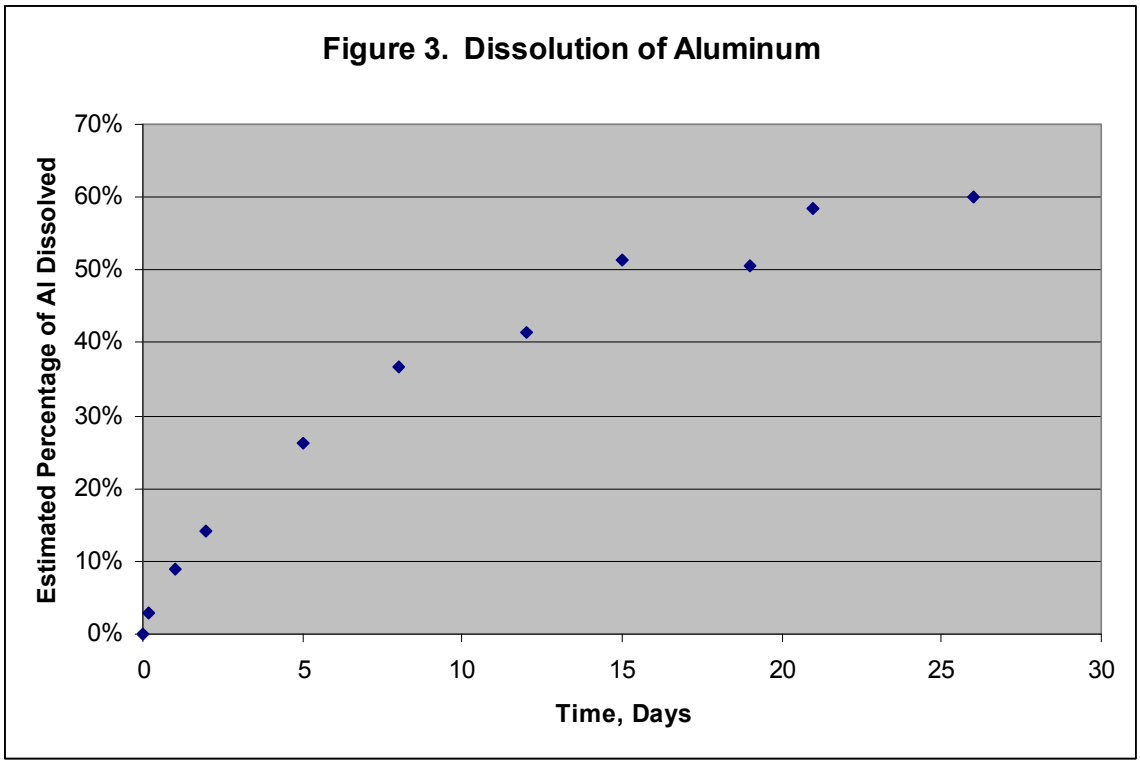

6.4.2 Iron

The concentration of Fe in solution increased by a factor of at least three or four over the duration of the dissolution period (from ~10 mg/L at the start of the dissolution period to 30 mg/L or more at the end of the period). Additionally, the Fe concentration increased by a factor of approximately three upon adding the caustic (from ~3 mg/L prior to the caustic addition to ~10 mg/L at time zero of the demonstration). The net effect was an order of magnitude increase (or more) due to dissolution. Note that the relatively high Fe concentrations observed at days 12, 21, and 25 were considered questionable, since they were sporadic and so much higher than the concentration observed following dissolution (21 mg/L). Possibly these high concentrations were due to colloidal Fe-containing particles that were released when Al structures dissolved and were smaller than the 0.45 μm pores of the filter membrane. Accurate quantification of Fe in standards analyzed alongside the leachates indicated that the elevated Fe concentrations in the leachates were not analytical anomalies.

Estimates of the percentages of Fe that were solubilized during the dissolution period are given in Figure 4. As shown in the figure, a maximum of ~1% of the Fe appeared to dissolve if the questionable data were neglected. On the other hand, a maximum of ~10% of the Fe appeared to dissolve if the questionable data were assumed valid. If the difference between one and ten percent of Fe dissolving is impactive, additional study of this phenomena should be pursued.

Figure 4. Dissolution of Iron

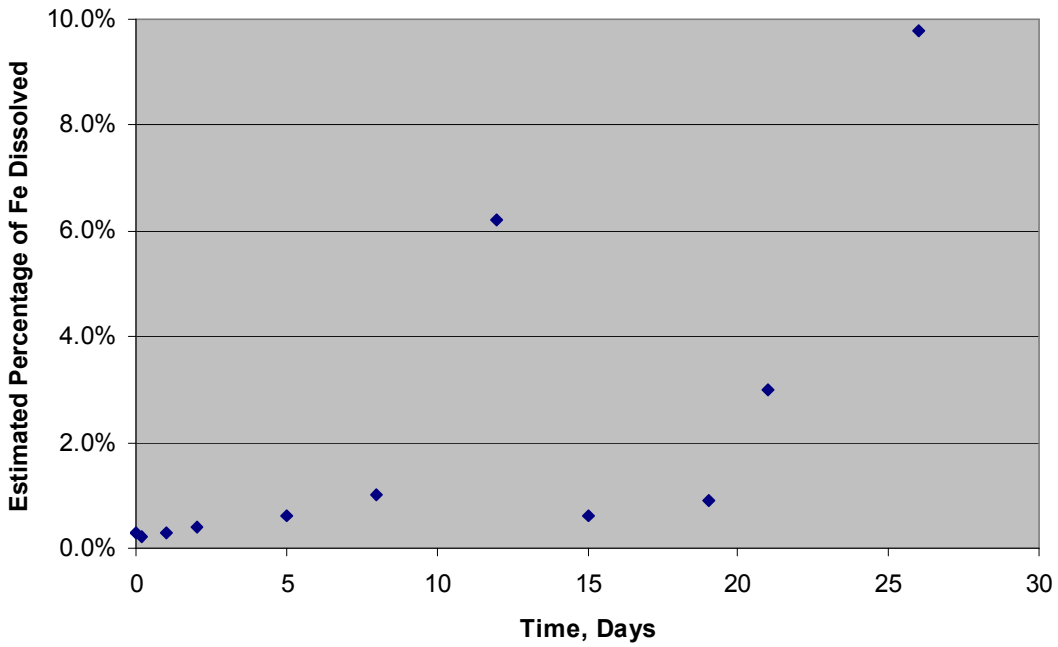

6.4.3 Gadolinium

All concentrations of Gd in solution were less than the analytical minimum detection limits. As a consequence, no conclusions can be drawn regarding the trend of Gd concentrations over the course of the dissolution period. However, upper bounds for the percentages of Gd dissolved could be determined and are given below in Table 7. As shown in the table, the upper bounds ranged from about 1-3%. Since the lowest upper bounds appeared at the conclusion of the dissolution period (where the quantity dissolved is expected to be highest), it is very likely that less than 1% of the Gd was in solution at all times during the dissolution period.

Table 7. Percentage of Gd Dissolved

Time, Days	Percentage of Gd Dissolved
0	<1.5
0.2	<1.5
1	<2.2
2	<1.1
5	<1.7
8	<2.8
12	<1.5
15	<2.2
19	<1.7
21	<1.0
26	<1.0

6.4.4 Uranium

The concentration of U in solution fluctuated up and down somewhat over the dissolution period, but remained the same order of magnitude throughout. The lowest concentration (5.4 mg/L) was seen at 19 days, while the highest concentration (11 mg/L) was seen at 4 hours. Results indicate that the U concentration increased by a factor of ~2 (from ~6 to 11 mg/L) four hours after the caustic was added and then returned to the starting concentration over the next week. A clear increase in U concentration was observed prior to dissolution, when the Pu/Gd solution was added to the slurry, which was expected based on the relatively high U content of the Pu/Gd stream. The slightly lower concentration observed in the post-dissolution supernatant (4.4 mg/L) may indicate that a small portion of the soluble U precipitated out of solution when the slurry was cooled.

Estimates of the percentages of U that were soluble during the dissolution period are given in Figure 5. As shown in the figure, the percentages were all minor, on the order of 1% or less.

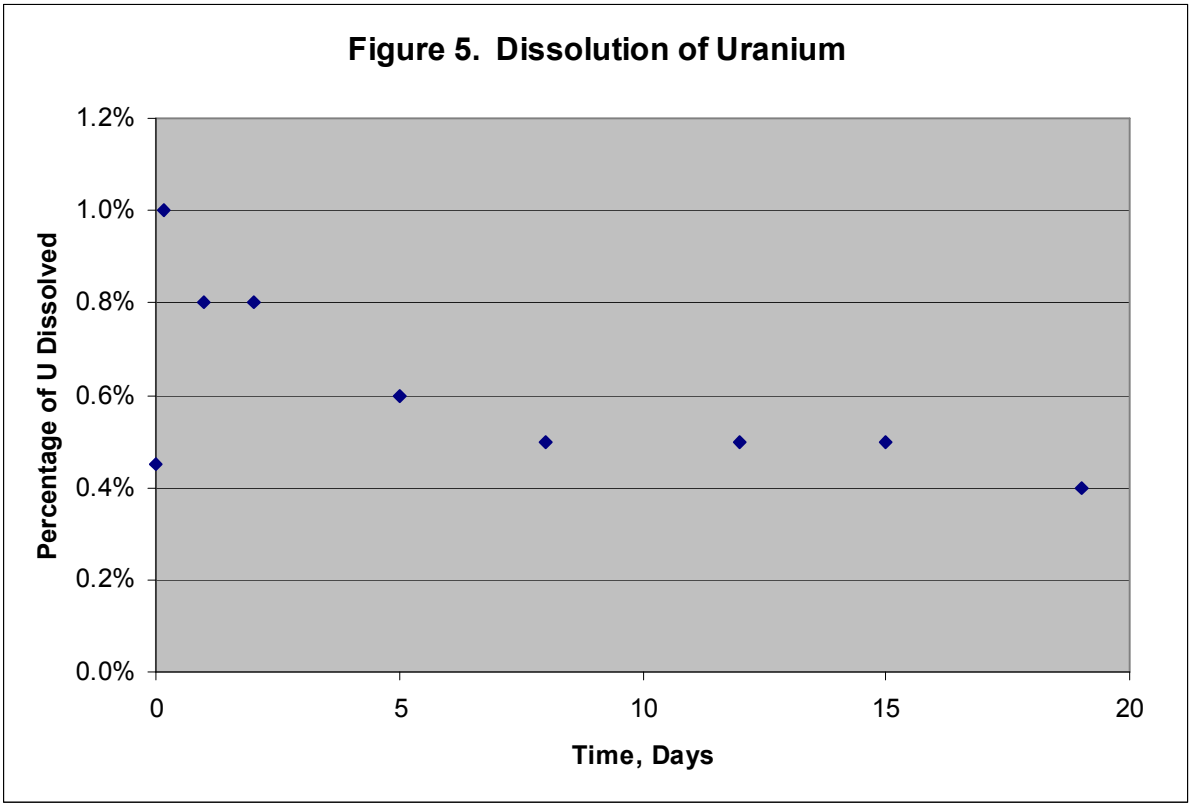

6.4.5 Plutonium

The concentrations of Pu-238 and Pu-239 in solution increased a factor of two to three within the first few hours after adding the caustic solution, and then stayed relatively constant over the remainder of the dissolution period. A more dramatic increase in soluble Pu was seen prior to dissolution when the Pu/Gd solution was added. As previously discussed, addition of the Pu/Gd raised the supernatant Pu-238 concentration by a factor of around six and the Pu-239 concentration by a factor between seven and fifty. The net result was that the concentration of Pu at the end of dissolution was about two orders of magnitude higher than that of the "as received" supernatant.

Estimates of the percentages of Pu that were soluble over the dissolution period are given in Figure 6. As shown in the figure, approximately 20% of the Pu was soluble over most of the dissolution period (from 4 hours on). In contrast, ~7% of the Pu was soluble at time zero (when the caustic was added). This indicates that ~13% of the insoluble Pu solubilized during the aluminum dissolution period. Note that the portion of Pu that solubilized in the previous aluminum dissolution demonstration[3] was approximately 10%.

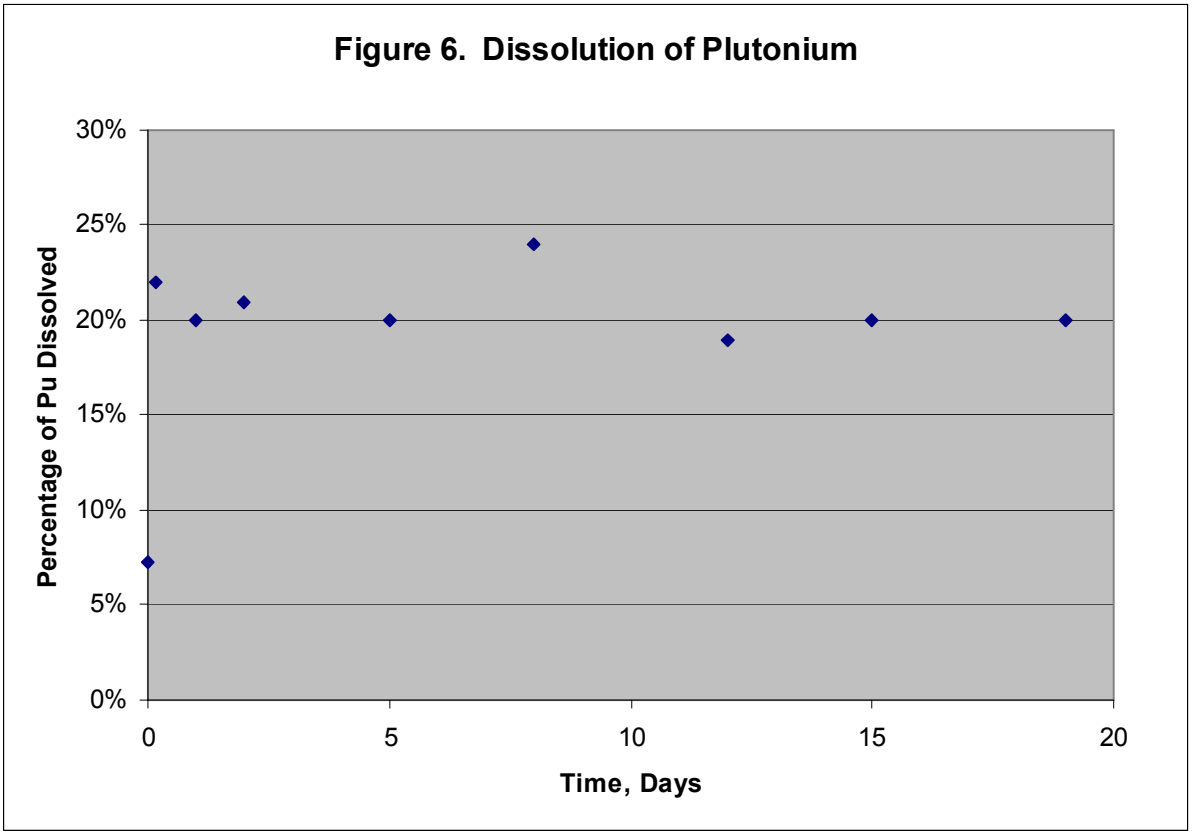

6.5 POST-DISSOLUTION SLURRY AND SUPERNATANT

Analytical results for the slurry and the supernatant of the post-dissolution slurry are given in Tables 8 and 9. These results indicate that the:

- Slurry and supernatant densities were 1.39 and 1.34 g/mL, respectively, slightly higher than those of the "as received" sample due to the higher caustic content
- Insoluble solids content was 4.4 wt%, ~60% of that of the "as received" slurry
- Soluble solids content was ~38 wt%, ~20% higher than the "as received" slurry
- Yield stress was 2.5 Pa, an order of magnitude lower than that of the "as received" slurry due to the lower insoluble solids content[16]
- Plastic viscosity was 27 cP, the same as that of the "as received" slurry
- Concentrations of most constituents (excluding those added with the Pu/Gd solution) were 70-80% of the concentrations in the "as received" slurry as expected due to dilution by the Pu/Gd and NaOH additions
- Concentrations of Cu, Gd, U, and Pu were higher due to the Pu/Gd addition
- Supernatant contained ~8 M Na^+, 5.1 M free OH^-, and 0.9 M $Al(OH)_4^-$. These concentrations are elevated from those of the "as received" supernatant, reflecting the effects of the added caustic and the dissolved aluminum
- The concentration of Hg in supernatant was 300 mg/L, which was ~35 times that of the "as received" supernatant (8.2 mg/L). This increase indicates dissolution of insoluble Hg, which is consistent with past behavior

Table 8. Analytical Results for Tank 12 Sludge Slurry After Aluminum Dissolution

Measurement	Method	Mean Result	*%RSD*
Density (g/mL)	VWM	1.39	*0.7*
Total solids (wt% of slurry)	WDW	42.0	*0.6*
Insoluble solids (wt% of slurry)	CLC	4.4	*NA*
Soluble solids (wt% of slurry)	CLC	37.6	*NA*
Yield stress (Pa)	RM	2.5	*1.0*
Plastic viscosity (cP)	RM	27	*0.9*
Aluminum (wt% of slurry)	PF/ICP-AES	3.0	*1.3*
Boron (wt% of slurry)	AR/ICP-AES	<0.0024	*NA*
Barium (wt% of slurry)	PF/ICP-AES	0.0059	*5.2*
Calcium (wt% of slurry)	AR/ICP-AES	0.084	*5.9*
Cerium (wt% of slurry)	AR/ICP-AES	<0.011	*NA*
Chromium (wt% of slurry)	PF/ICP-AES	0.035	*13*
Copper (wt% of slurry)	PF/ICP-AES	0.016	*1.7*
Gadolinium (wt% of slurry)	AR/ICP-MS	0.0046	*3.0*
Iron (wt% of slurry)	PF/ICP-AES	0.42	*8.2*
Lanthanum (wt% of slurry)	AR/ICP-AES	0.0030	*2.6*
Magnesium (wt% of slurry)	AR/ICP-AES	0.0080	*6.1*
Manganese (wt% of slurry)	PF/ICP-AES	0.14	*2.8*
Mercury (wt% of slurry)	AR/AA	0.10	*2.4*
Molybdenum (wt% of slurry)	AR/ICP-AES	<0.0067	*NA*
Nickel (wt% of slurry)	PF/ICP-AES	0.046	*3.3*
Palladium (wt% of slurry)	AR/ICP-MS	<9.7E-4	*NA*
Potassium (wt% of slurry)	AR/ICP-AES	0.059	*7.4*
Ruthenium (wt% of slurry)	AR/ICP-MS	0.0046	*13*
Rhodium (wt% of slurry)	AR/ICP-MS	9.2E-4	*16*
Silicon (wt% of slurry)	AR/ICP-AES	<0.016	*NA*
Silver (wt% of slurry)	AR/ICP-AES	<0.0042	*NA*
Sodium (wt% of slurry)	AR/ICP-AES	16	*0.5*
Strontium (wt% of slurry)	AR/ICP-AES	0.0017	*1.7*
Thorium (wt% of slurry)	AR/ICP-MS	0.036	*3.2*
Titanium (wt% of slurry)	AR/ICP-AES	<0.0013	*NA*
Uranium (wt% of slurry)	AR/ICP-MS	0.018	*2.6*
Zinc (wt% of slurry)	AR/ICP-AES	0.0042	*3.1*
Zirconium (wt% of slurry)	AR/ICP-AES	0.013	*5.3*
Total alpha (Ci/gallon)	PF/LSC	<0.42	*NA*
Total beta (Ci/gallon)	PF/LSC	8.5	*2.7*
Co-60 (Ci/gallon)	PF/GS	1.3E-4	*6.7*
Tc-99 (Ci/gallon)	AR/ICP-MS	6.2E-4	*11*
Cs-137 (Ci/gallon)	PF/GS	0.79	*3.3*
Ba-137m (Ci/gallon)	PF/GS	0.74	*3.3*
Eu-152 (Ci/gallon)	PF/GS	7.0E-4	*7.1*
Eu-154 (Ci/gallon)	PF/GS	0.0091	*2.0*
Eu-155 (Ci/gallon)	PF/GS	6.4E-4	*16*
U-235 (Ci/gallon)	AR/ICP-MS	1.9E-7	*11*
U-238 (Ci/gallon)	AR/ICP-MS	2.9E-7	*3.5*
Np-237 (Ci/gallon)	AR/ICP-MS	<7.0E-6	*NA*
Pu-238 (Ci/gallon)	PF/AS	0.23	*3.8*
Pu-239 (Ci/gallon)	AR/ICP-MS	0.018	*4.6*
Pu-239/240 (Ci/gallon)	PF/AS	0.024	*5.1*
Pu-241 (Ci/gallon)	PF/LSC	0.079	*2.8*
Am-241 (Ci/gallon)	PF/GS	0.014	*2.1*

Table 9. Analytical Results for Filtered Supernatant of Tank 12 Slurry Following Aluminum Dissolution But Prior to Settling

Measurement	Method	Mean Result	*%RSD*
Density (g/mL)	VWM	1.34	*0.5*
Dissolved solids (wt% of supernatant)	WDW	39.4	*0.3*
Aluminum (mg/L)	ICP-AES	2.4E+4	*0.2*
Boron (mg/L)	ICP-AES	<61	*NA*
Barium (mg/L)	ICP-AES	<4.0	*NA*
Calcium (mg/L)	ICP-AES	19	*12*
Cerium (mg/L)	ICP-AES	<50	*NA*
Chromium (mg/L)	ICP-AES	90	*0.6*
Copper (mg/L)	ICP-AES	1.1E+2	*1.0*
Gadolinium (mg/L)	ICP-MS	<1.7	*NA*
Iron (mg/L)	ICP-AES	<1.0E+2	*NA*
Lanthanum (mg/L)	ICP-AES	<44	*NA*
Magnesium (mg/L)	ICP-AES	<8.6	*NA*
Manganese (mg/L)	ICP-AES	<26	*NA*
Mercury (mg/L)	AA	3.0E+2	*3.9*
Molybdenum (mg/L)	ICP-AES	<1.7E+2	*NA*
Nickel (mg/L)	ICP-AES	<50	*NA*
Palladium (mg/L)	ICP-MS	1.3	*11*
Potassium (mg/L)	ICP-AES	5.2E+2	*4.1*
Ruthenium (mg/L)	ICP-MS	<1.3	*NA*
Rhodium (mg/L)	ICP-MS	1.6	*10*
Silicon (mg/L)	ICP-AES	<48	*NA*
Silver (mg/L)	ICP-AES	<11	*NA*
Sodium (mg/L)	ICP-AES	1.8E+5	*0.4*
Strontium (mg/L)	ICP-AES	<4.0	*NA*
Thorium (mg/L)	ICP-MS	<1.8	*NA*
Titanium (mg/L)	ICP-AES	<19	*NA*
Uranium (mg/L)	ICP-MS	4.7	*8.9*
Zinc (mg/L)	ICP-AES	19	*9.3*
Zirconium (mg/L)	ICP-AES	<25	*NA*
Tc-99 (Ci/gallon)	ICP-MS	2.0E-4	*3.3*
Sn-126 (Ci/gallon)	GS	<2.7E-5	*NA*
Sb-126 (Ci/gallon)	GS	<2.7E-5	*NA*
Cs-137 (Ci/gallon)	GS	0.72	*4.3*
Ba-137m (Ci/gallon)	GS	0.67	*4.3*
U-235 (Ci/gallon)	ICP-MS	3.6E-9	*12*
U-238 (Ci/gallon)	ICP-MS	5.6E-9	*14*
Np-237 (Ci/gallon)	ICP-MS	<5.1E-7	*NA*
Pu-238 (Ci/gallon)	AS	0.0062	*10*
Pu-239 (Ci/gallon)	ICP-MS	0.0028	*2.6*
Pu-239/240 (Ci/gallon)	AS	0.0039	*21*
Pu-241 (Ci/gallon)	LSC	<0.0075	*NA*
Sodium (M)	ICP-AES	7.83	*0.4*
Potassium (M)	ICP-AES	0.013	*4.1*
Free hydroxide (M)	BT	5.05	*1.0*
Nitrite (M)	IC	1.23	*1.3*
Nitrate (M)	IC	1.34	*1.6*
Carbonate (M)	TIC	0.28	*0.5*
Aluminate (M)	ICP-AES	0.89	*0.2*
Chloride (M)	IC	<0.035	*NA*
Sulfate (M)	IC	0.041	*0.2*
Fluoride (M)	IC	<0.065	*NA*
Formate (M)	IC	<0.027	*NA*
Phosphate (M)	IC	<0.013	*NA*
Oxalate (M)	IC	<0.014	*NA*

Differences in the masses of Pu-239 and Gd before and after aluminum dissolution were calculated based on the analytical results. As summarized in Table 10, the measured results for Pu-239 were 0.0073 Ci/gal for the "as received" slurry and 0.018 Ci/gal for the post-dissolution slurry. The difference on a Ci/gal basis is ~0.011. Using the mass balance of the demonstration, this difference equates to a Pu-239 mass addition of 0.18 g. This mass agrees well with expectations, as the targeted Pu-239 addition was 0.19 g.

Table 10. Measurements of Pu-239 and Gd in "As Received" and Post-Dissolution Slurries

Constituent	As Received	Post-dissolution	Measured Difference in Mass
Pu-239	0.0073 Ci/gal	0.018 Ci/gal	0.18 g
Gd	0.000010 wt%	0.0046 wt%	0.21 g

Similarly, the difference between the Gd concentration of the "as received" slurry (0.000010 wt%) and the post-dissolution slurry (0.0046 wt%) is ~0.0046 wt%. Using the mass balance, this difference equates to a Gd mass addition of 0.21 g. As in the case of the Pu-239, the measured Gd increase agrees well with expectations (the targeted Gd addition was 0.19 g). These comparisons provide confidence that the Pu/Gd addition was executed effectively.

Ratios of constituent concentrations in the post-dissolution slurry to constituent concentrations in the "as received" slurry are given in Table 11, along with comments addressing the implications of the ratios. This information is provided to facilitate understanding of the data. Not all constituents are addressed in the table – constituents whose concentrations are below detection limits and/or whose role is of questionable pertinence were omitted. Note that the typical concentration ratio for constituents affected solely by dilution (due to Pu/Gd/NaOH additions) is ~0.7 to 0.8.

Similarly, ratios of constituent concentrations in the post-dissolution supernatant to constituent concentrations in the "as received" supernatant are given in Table 12.

6.6 SLUDGE SETTLING

The settling behavior of the post-dissolution sludge is plotted as a function of time in Figure 7. As shown in the figure, the settling rate was relatively rapid over the first few days, but then significantly slower over the following two to three weeks. Although settling of the post-dissolution slurry was markedly quicker than that of the "as received" slurry (Figure 2), it was clearly slower than that of typical high-iron content/low salt content sludges. As mentioned in Section 5.5, the post-dissolution supernatant was greenish-grey in color. This color combined with the semi-opaque appearance of the dissolution vessel walls added uncertainty to the settling measurements, as it made discernment of the interface between the settled sludge and free supernatant layers less clear.

Table 11. "Post-dissolution" to "As Received" Slurry Constituent Concentration Ratios

Slurry Constituent	Concentration Ratio (Post-diss:As-rec'd)	Comments
Aluminum	0.70	Reflects dilution from Pu/Gd/NaOH sol'ns
Copper	4.1	Reflects Cu added with Pu/Gd solution
Gadolinium	460	Reflects Gd added with Pu/Gd solution
Iron	1.1	Reflects analytical uncertainty (AU)
Manganese	0.78	Reflects dilution from Pu/Gd/NaOH sol'ns
Mercury	0.67	Reflects dilution from Pu/Gd/NaOH sol'ns
Nickel	1.0	Reflects AU
Potassium	1.3	Reflects K added with Pu/Gd
Sodium	1.3	Reflects Na added with alkalized Pu/Gd
Thorium	0.40	Suggests elevated AU
Uranium	1.8	Reflects U added with Pu/Gd
Zinc	0.78	Reflects dilution from Pu/Gd/NaOH sol'ns
Zirconium	0.76	Reflects dilution from Pu/Gd/NaOH sol'ns
Total beta	0.77	Reflects dilution from Pu/Gd/NaOH sol'ns
Cs-137	0.66	Reflects AU and dilution from Pu/Gd/NaOH sol'ns
U-235	1.6	Reflects U-235 added with Pu/Gd solution
U-238	1.9	Reflects U-238 added with Pu/Gd solution
Pu-238	0.88	Reflects AU
Pu-239	2.5	Reflects Pu-239 added with Pu/Gd solution
Pu-239/240	3.8	Reflects Pu-239 and Pu-240 added with Pu/Gd sol'n

Table 12. "Post-dissolution" to "As Received" Supernatant Constituent Concentration Ratios

Supernatant Constituent	Concentration Ratio (Post-diss:As-rec'd)	Comments
Aluminum	2.2	Reflects dissolution of Al
Iron	7.0	Reflects dissolution of Fe
Mercury	37	Reflects dissolution of Hg
Potassium	0.78	Reflects dilution from Pu/Gd/NaOH sol'ns
Sodium	1.1	Reflects soluble Na added with NaOH sol'n
Uranium	2.0	Reflects effects of Pu/Gd sol'n
Zinc	5.8	Reflects dissolution of Zn
Cs-137	2.2	Reflects dissolution of Cs
Pu-238	20	Reflects effects of Pu/Gd sol'n and dissolution
Pu-239	>58	Reflects effects of Pu/Gd sol'n and dissolution
Pu-239/240	443	Reflects effects of Pu/Gd sol'n and dissolution
Free $(OH)^-$	7.7	Reflects NaOH addition
Nitrite	0.70	Reflects dilution from Pu/Gd/NaOH sol'ns
Nitrate	0.91	Reflects AU and dilution from Pu/Gd/NaOH sol'ns
Carbonate	0.34	Reflects precipitation of carbonate salt(s)
Sulfate	0.80	Reflects dilution from Pu/Gd/NaOH sol'ns

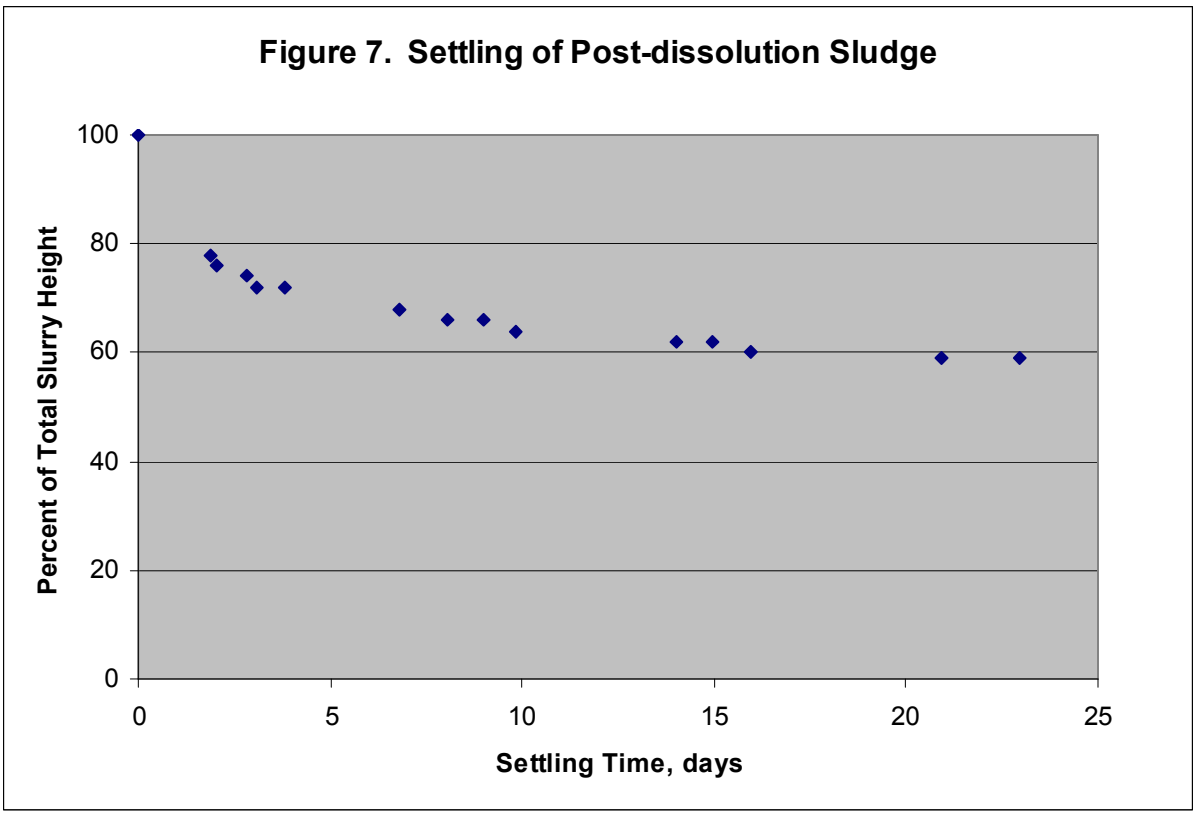

6.7 POST-SETTLING DECANT SOLUTION

The volume of supernatant decanted from the settled waste solution was approximately 35% of the total waste volume. As mentioned before, the post-dissolution supernatant exhibited a greenish-grey hue, which when viewed through the walls of the HDPE dissolution vessel appeared relatively dark. However, when viewed in a clear glass beaker, the color of the supernatant appeared significantly lighter, as shown in Figure 8. For the sake of comparison, a photograph of the decant solution in the HDPE vessel alongside the decant solution in the glass beaker is given in Figure 9. Based on the relative clarity of the solution as seen in the beaker, it is expected that a turbidity measurement of the supernatant would provide a significantly different result than one of a settled sludge layer.

Figure 8. Post-Settling Decant Solution in a 30 mL Glass Beaker

Figure 9. Post-Settling Decant Solution in an HDPE Vessel and a Glass Beaker

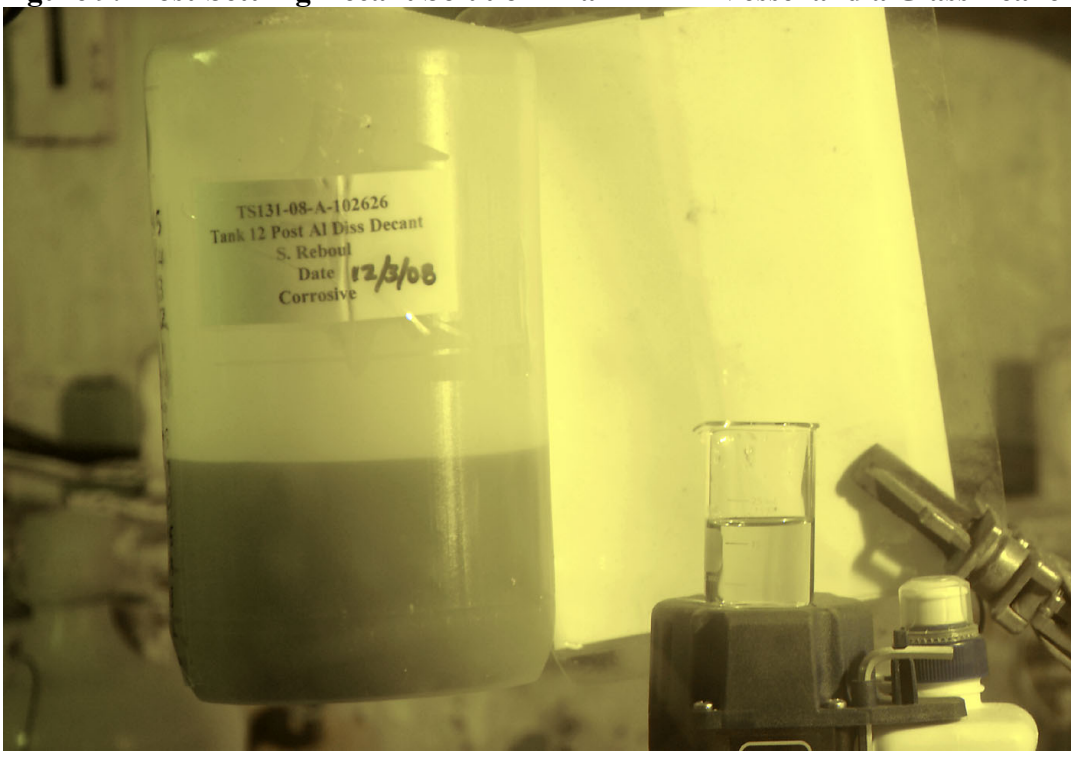

Analytical results for the post-settling filtered decant solution are given in Table 13. These results indicate a metals content similar to that of the pre-settling filtered supernatant. For Al, Cr, Na, and Zn, the concentration differences between the two solutions were less than 20%, which was considered minor, as it was the same magnitude as the assumed analytical uncertainty. For Cu and K, the differences were somewhat higher (30% for Cu and 37% for K), although still of a magnitude reflecting similar content. The biggest difference was observed for Ca, with a post-settling concentration 60% lower than that of the pre-settling supernatant. Detectable concentrations of Ca in supernatant "blanks" suggested this difference may have been due to Ca in the diluent solutions which biased the Ca results high, especially in the pre-settling case where a greater dilution factor was utilized. Another possibility to account for the difference is that some portion of the Ca may have precipitated out of solution during the settling period. With exception of the Ca case, all detectable metal concentrations in the post-settling decant agreed well with those of the pre-settling supernatant. This agreement indicates that partitioning changes during the settling period were generally minor or insignificant. Based on the Al concentration (2.8E+4 mg/L) and the volume of supernatant that was decanted (Section 5.6), approximately one-third of the dissolved aluminum was removed in the decant.

Table 13. ICP-AES Results for Post-Dissolution/Post-Settling Filtered Decant Solution

Measured Analyte	Mean Result, mg/L	*%RSD*
Aluminum	2.8E+4	*0.2*
Boron	33	*0.5*
Barium	<0.64	*NA*
Calcium	7.3	*16*
Cerium	<10	*NA*
Chromium	100	*0.2*
Copper	140	*0.5*
Gadolinium	<3.5	*NA*
Iron	21	*15*
Lanthanum	<2.0	*NA*
Magnesium	<18	*NA*
Manganese	<0.67	*NA*
Molybdenum	32	*1.6*
Nickel	<4.3	*NA*
Potassium	710	*2.1*
Silicon	<16	*NA*
Silver	<3.5	*NA*
Sodium	2.1E+5	*0.3*
Strontium	<1.5	*NA*
Titanium	<0.5	*NA*
Uranium	<70	*NA*
Zinc	18	*9.3*
Zirconium	<0.64	*NA*

7.0 CONCLUSIONS

1) Aluminum was the predominant constituent of the "as received" sludge and was present in the form of boehmite. Concentrations of iron, manganese, and nickel were one or more orders of magnitude lower than the aluminum concentration, and the Al:Fe and Fe:Mn mass ratios were clearly different from those of previous sludge batches. The salt content of the supernatant was relatively high, with a sodium concentration of ~7 M. Because of these characteristics, the yield stress of the slurry was relatively high and the settling rate of the sludge was low.

2) Approximately 60% of the insoluble aluminum dissolved over the 26 day demonstration period, with the rate of dissolution slowing significantly by the end of the demonstration. A consequence of the dissolution was a significantly reduced sludge yield stress (by an order of magnitude). Since the yield stress is likely a function of the insoluble solids content, it is anticipated that the yield stress after washing and decanting will still be high. However, direct measurements of washed/decanted post-dissolution sludge would be necessary to estimate the increase associated with concentrating the insolubles. Another consequence of the dissolution was a somewhat increased sludge settling rate (by a factor of about two). However, the settling rate slowed significantly after about two weeks, yielding barely discernible additional settling over the third week. The net effect was that the volume of decanted supernatant was only about 35% of the total waste volume. The decanted supernatant contained approximately one-third of the dissolved aluminum and was mildly greenish-grey in color.

3) Addition of the Pu/Gd solution to the Tank 12 sample raised the supernatant Pu concentration by one to two orders of magnitude. Aluminum dissolution raised the supernatant Pu concentration another order of magnitude. The net effect was that the portion of Pu in solution increased from ~0.1% for the "as received" slurry to ~20% for the post-dissolution slurry. In contrast, the total amount of Gd that partitioned to the liquid phase was minor (≤1%).

4) The portion of Fe that partitioned to the liquid phase appeared to be ~1% based on the majority of data. However, a minor part of the data suggested the partitioning could be as high as 10%. Additional testing would be needed to quantify the partitioning more definitively.

8.0 RECOMMENDATIONS

1) Rheology measurements of washed/decanted post-dissolution sludge as a function of insoluble solids content are recommended to better understand the range of yield stresses and plastic viscosities associated with Sludge Batch 6 material.

2) The potential impacts of solubilizing plutonium should be assessed to determine the acceptability of receiving plutonium discards immediately prior to aluminum dissolution.

3) Further study of iron solubility at high caustic concentrations is recommended to better quantify solid-liquid phase partitioning of iron during aluminum dissolution.

9.0 REFERENCES

1. Pike, J. A. *Preliminary Process Parameters for Aluminum Dissolution*, CBU-PIT-2006-00082, May 2006.

2. Hay, M. S.; Pareizs, J. M.; Bannochie, C. J.; Stone, M. E.; Click, D. R.; McCabe, D. J. *Preliminary Data from the 3L Tank 51H Aluminum Dissolution Test*, SRNL-CST-2007-00102, October 2007.

3. Hay, M. S.; Pareizs, J. M.; Bannochie, C. J.; Stone, M. E.; Click, D. R.; McCabe, D. J. *Characterization and Aluminum Dissolution Demonstration with a 3 Liter Tank 51H Sample*, WSRC-STI-2007-00697, February 2008.

4. Pareizs, J. M.; Bannochie, C. J.; Click, D. R.; Hansen, E. K.; Lambert, D. P.; Stone, M. E. *Washing and Demonstration of the DWPF Flowsheet in the SRNL Shielded Cells Using Post Aluminum Dissolution Tank 51 Sludge Slurry*, WSRC-STI-2008-00086, April 2008.

5. Pike, J. A. *Preliminary Results for Low Temperature Aluminum Removal from Sludge Batch 5*, LWO-LWE-2008-00067, March 2008.

6. Pike, J. A.; Johns, N. A. *In Process Sample Results for Low-Temperature Aluminum Dissolution*, LWO-LWE-2008-00050, March 2008.

7. Hay, M. S.; McCabe, D. J. *Characterization of Tank 11H and Tank 51H Post Aluminum Dissolution Process Samples*, WSRC-STI-2008-00227, May 2008.

8. Ketusky, E. T. *Tank 12 Characterization and Aluminum Dissolution Demonstration*, HLE-TTR-2008-52, Rev. 1, August 2008.

9. Reboul, S. H., K. E. Zeigler, and M. S. Hay. *Task Technical and Quality Assurance Plan: Tank 12 Characterization and Aluminum Dissolution Demonstration*, SRNS-RP-2008-00156.

10. Hay, M. S. *Laboratory Notebook: Tank Waste Testing*, WSRC-NB-2008-00077, Date Opened: July 28, 2008.

11. Reboul, S. H. *Laboratory Notebook: Tank 12 Aluminum Dissolution Demonstration*, WSRC-NB-2008-00078, Date Opened: July 29, 2008.

12. Reboul, S. H. *Laboratory Notebook: Tank 12 Aluminum Dissolution Demonstration Part 2*, SRNL-NB-2009-00021, Date Opened: February 2, 2009.

13. Reboul, S. H., K. E. Zeigler, and M. S. Hay. *Tank 12 Characterization and Aluminum Dissolution Demonstration: Analytical Study Plan*, SRNL-RP-2008-00171, September 23, 2008.

14. United States Department of Energy. *Plutonium Disposition Alternative Analysis*, Y-AES-G-00001, Rev. 1, March 2008.

15. Pike, J. A. *Email message to S. H. Reboul with subject heading of "Re: schedule*," 11:52 a.m. on October 9, 2008 (see Appendix A).

16. Reboul, S. H. *Solids, Density, and Rheology of Tank 12 Sludge Blends*, SRNL-L3100-2009-00036, February 12, 2009.

10.0 ACKNOWLEDGEMENTS

The following individuals are acknowledged for contributing to this study: Lucy Beasley, Debbie Burckhalter, Phyllis Burkhalter, Mona Galloway, Jane Howard, Monica Jenkins, Nan Stanley, Rita Sullivan, and Dee Wheeler, who performed the sample preparations and analyses in the Shielded Cells; Mike Bronikowski, who generated the Pu/Gd doping solution; Mark Jones, who performed the ICP-AES analyses; Curtis Johnson, who performed the ICP-MS and AA analyses; David and CeCi DiPrete, who performed the radiochemical analyses; Kathy White, who performed the TIC and BT analyses; Boyd Wiedenman, who performed the IC analyses; Art Jurgensen, who performed the XRD analyses; Leigh Brown, who coordinated the AD analyses; and Erich Hansen, who provided technical support on the RM analyses.

APPENDIX A: FLOWSHEET MODELING RESULTS

Jeff Pike/SRNL/Srs
10/09/2008 11:52 AM

To Scott Reboul/SRNL/Srs@Srs
cc Daniel McCabe/SRNL/Srs@Srs, Michael Hay/SRNL/Srs@Srs
bcc
Subject Re: schedule

History: This message has been forwarded.

I updated the material balance to account for the slight dilution of solids by the Pu/Gd addition and based the calculation on 2.5 L of initial slurry. The target OH drops to 5.0 M and the ratio of OH to Al in the solids is now 4.4. Effectively, the endpoint moves down somewhat from the steepest part of the solubility curve.

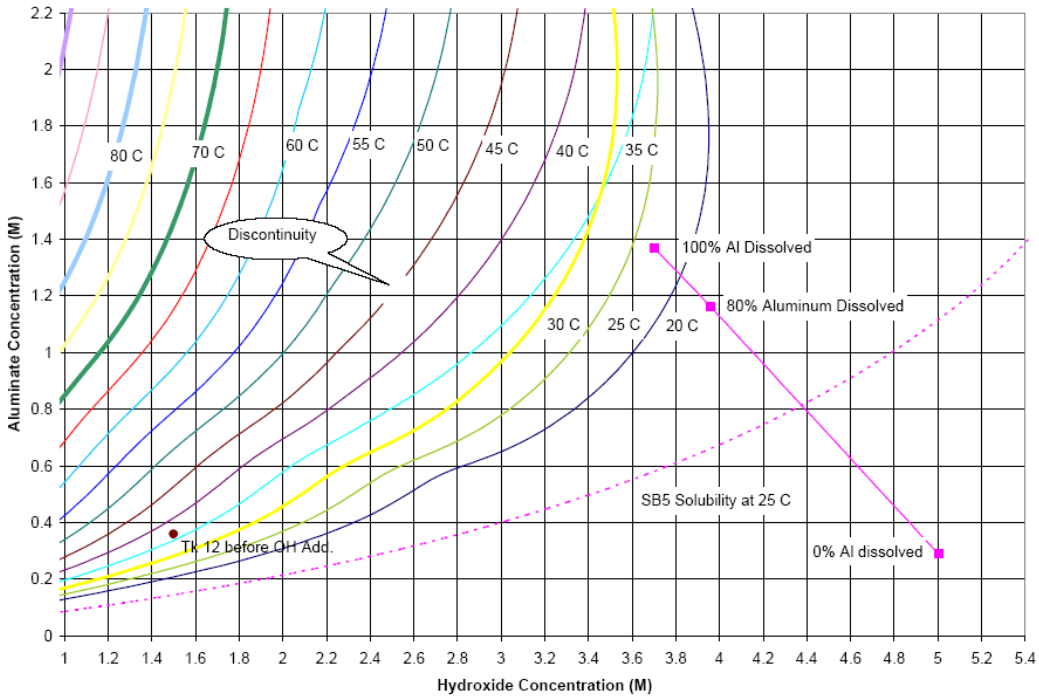

APPENDIX A: FLOWSHEET MODELING RESULTS (CONT'D)

	Before		After Pu/Gd	NaOH Addition	Before Dissolution	After Dissolution	80% After Dissolution	100% After Dissolution
Na+ (measured)	7.05		6.84					
Na+	6.97		6.75	19.53	9.31	9.01		8.92
NO2-	1.76		1.62	0	1.30	1.26		1.25
NO3-	1.47		1.60	0	1.29	1.25		1.23
OH-	1.53		1.50	19.1	5.00	3.96		3.70
Cl-	0.025		0.023	0.43	0.10	0.10		0.10
SO4-	0.051		0.047	0	0.038	0.037		0.036
F-	0.0027		0.0027	0	0.0022	0.0021		0.0021
CO3-2	0.83		0.76	0	0.61	0.59		0.59
AlO2-	0.39		0.36	0	0.29	1.16		1.37
C2O4-2	0.0078		0.0078	0	0.0063	0.0061		0.0060
PO4-3	0.00501		0.00501	0	0.0040	0.0039		0.0039
K+	0.017		0.016	0	0.0129	0.0125		0.0123
Slurry Vol (L)	2.5	0.25	2.750	0.675	3.412	3.515		3.548
wt% Insoluble Solids	7.20%		6.41%		5.04%	1.19%		0.22%
Sp G	1.35		1.38		1.41	1.37		1.36
Mass Slurry (kg)	3.375		3.790	1.033	4.822	4.822		4.822
Liquid Phase								
Liquid Vol (L)	2.4857	0.2500	2.736	0.675	3.3979	3.5115		3.5475
Sp G	1.260		1.296	1.530	1.348	1.357		1.356
Mass of liquid, kg	3.132		3.5467	1.0328	4.5795	4.7653		4.8118
Al, kg	0.0262		0.0266		0.0266	0.1102		0.1311
Solid Phase								
Solids Vol (L)	0.0143		0.0143		0.0143	0.0034		0.0006
Sp G (bulk-hydrated)	17.01		17.01		17.01	17.01		17.01
Mass of Insoluble Solids, kg, dried solids	0.2430		0.2430		0.2430	0.0572		0.0107
wt% Al in insoluble solids	43%		43%		43%	37%		0%
wt% $Al(OH)_3$ in insoluble solids	124%		124%		124%	106%		0%
wt% AlO(OH) in insoluble solids	96%		96%		96%	81%		0%
Al, kg (as elemental Al)	0.1045		0.1045		0.1045	0.0209		0.0000
Other than Al Components, kg	0.1385		0.1385		0.1385	0.0363		0.0107

APPENDIX B: SPECIATION OF INSOLUBLE ALUMINUM BASED ON DISSOLUTION RATE

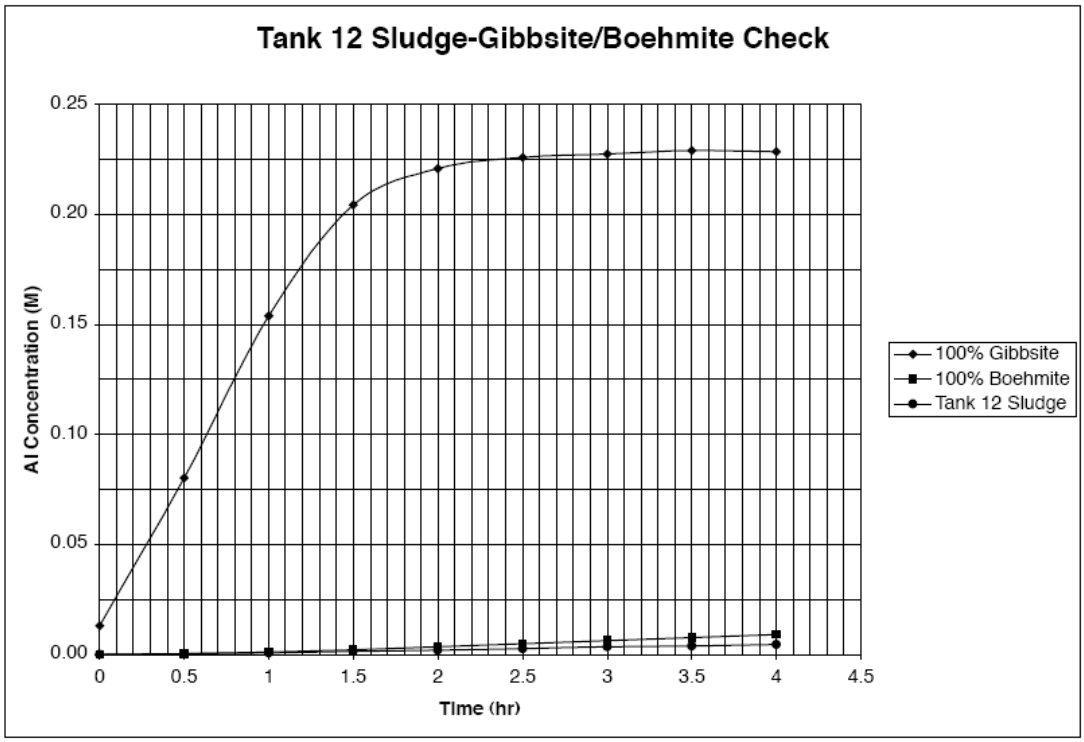

APPENDIX C: XRD SPECTRA FOR WASHED INSOLUBLE SOLIDS

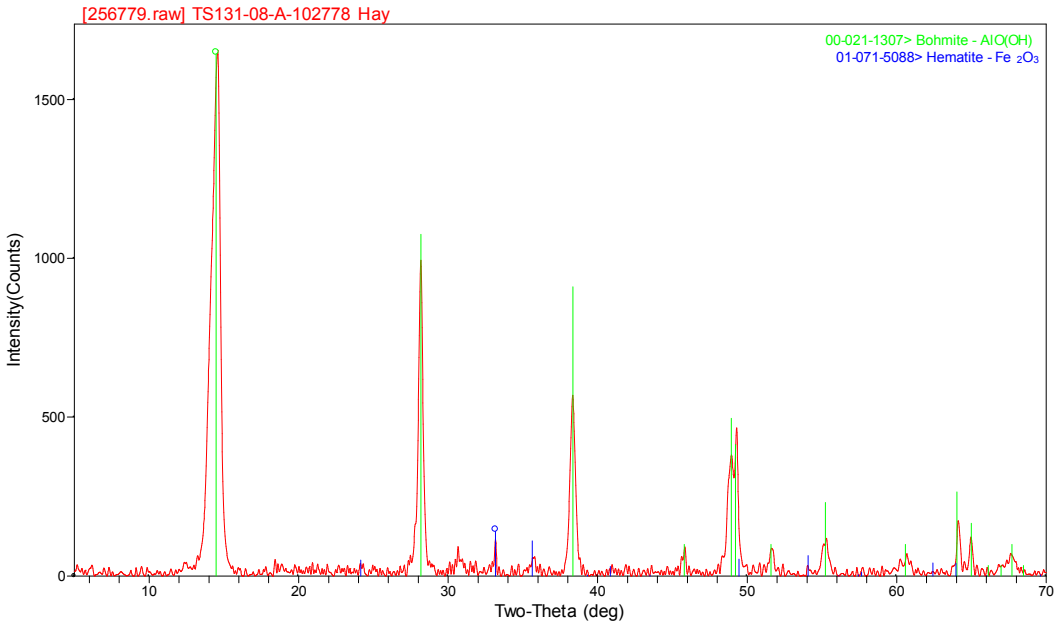

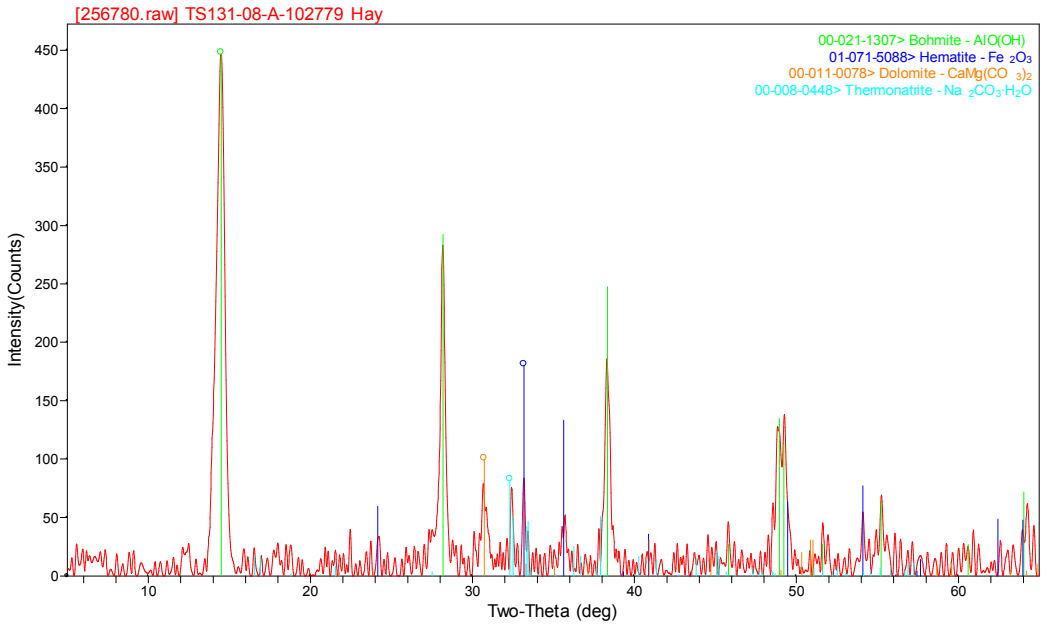

Distribution:

S. L. Marra, 773-A
A. B. Barnes, 999-W
D. A. Crowley, 773-43A
S. D. Fink, 773-A
C. W. Gardner, 773-A
B. J. Giddings, 786-5A
C. C. Herman, 999-W
F. M. Pennebaker, 773-42A
J. E. Occhipinti, 704-S
D. C. Sherburne, 704-S
R. T. McNew, 704-27S
J. F. Iaukea, 704-30S
J. W. Ray, 704-S
H. B. Shah, 766-H
J. C. Griffin, 773-A
J. M. Gillam, 766-H
B. A. Hamm, 766-H
D. D. Larsen, 766-H
C. J. Bannochie, 773-42A
D. J. McCabe, 773-42A
D. K. Peeler, 999-W
J. M. Bricker, 704-27S
T. L. Fellinger, 704-26S
E. W. Holtzscheiter, 704-15S
M. T. Keefer, 766-H
M. D. Buxton, 241-156H
M. Hubbard, 241-162H
A. J. Tisler, 704-61H
T. B. Caldwell, 766-H
P. J. Hill, 766-H
C. M. Cole, 704-61H
M. N. Borders, 704-56H
E. K. Hansen, 999-W
M. J. Ades, 704-60H
P. N. Bhatt, 241-162H
D. C. Bumgardner, 704-56H
K. B. Martin, 704-60H
A. W. Wiggins, 704-60H
D. J. Clark, 241-162H
J. A. Pike, 773-42A
H. H. Elder, 704-26S
Q. L. Nguyen, 704-60H
A. S. Choi, 773-42A
J. R. Zemecnik, 999-W
D. P. Lambert, 999-W
K. M. Fox, 999-W
D. C. Koopman, 999-W
N. E. Bibler, 773-A
A. I. Fernandez, 999-W
N. C. Iyer, 773-41A
M. J. Barnes, 773-A
M. G. Bronikowski, 773-A
K. E. Zeigler, 773-41A
M. S. Hay, 773-42A
J. M. Pareizs, 773-A
S. H. Reboul, 773-42A
M. E. Stone, 999-W